Journal Pre-proof

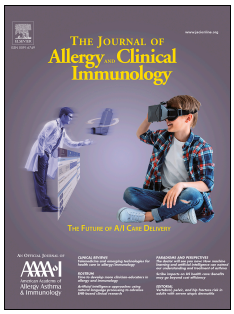

A Group of Cationic Amphiphilic Drugs Activates MRGPRX2 and Induces Scratching Behavior in Mice

Katharina Wolf, PhD, Helen Kühn, PhD, Felicitas Boehm, MSc, Lisa Gebhardt, MSc, Markus Glaudo, MSc, Konstantin Agelopoulos, PhD, Sonja Ständer, MD, Philipp Ectors, PhD, Dirk Zahn, PhD, Yvonne K. Riedel, MSc, Dominik Thimm, PhD, Christa E. Müller, PhD, Sascha Kretschmann, PhD, Anita N. Kremer, MD, PhD, Daphne Chien, BSc, Nathachit Limjunyawong, PhD, Qi Peng, Xinzhong Dong, PhD, Pavel Kolkhir, MD, Jörg Scheffel, PhD, Mia Lykke Søgaard, MSc, Benno Weigmann, PhD, Markus F. Neurath, MD, Tomasz Hawro, MD, PhD, Martin Metz, MD, Michael J.M. Fischer, MD, Andreas E. Kremer, MD, PhD

PII: S0091-6749(21)00229-3

DOI: https://doi.org/10.1016/j.jaci.2020.12.655

Reference: YMAI 14983

To appear in: *Journal of Allergy and Clinical Immunology*

Received Date: 28 April 2020

Revised Date: 10 November 2020

Accepted Date: 28 December 2020

Please cite this article as: Wolf K, Kühn H, Boehm F, Gebhardt L, Glaudo M, Agelopoulos K, Ständer S, Ectors P, Zahn D, Riedel YK, Thimm D, Müller CE, Kretschmann S, Kremer AN, Chien D, Limjunyawong N, Peng Q, Dong X, Kolkhir P, Scheffel J, Søgaard ML, Weigmann B, Neurath MF, Hawro T, Metz M, Fischer MJM, Kremer AE, A Group of Cationic Amphiphilic Drugs Activates MRGPRX2 and Induces Scratching Behavior in Mice, *Journal of Allergy and Clinical Immunology* (2021), doi: https://doi.org/10.1016/j.jaci.2020.12.655.

A Group of Cationic Amphiphilic Drugs Activates MRGPRX2 and Induces Scratching Behavior in Mice

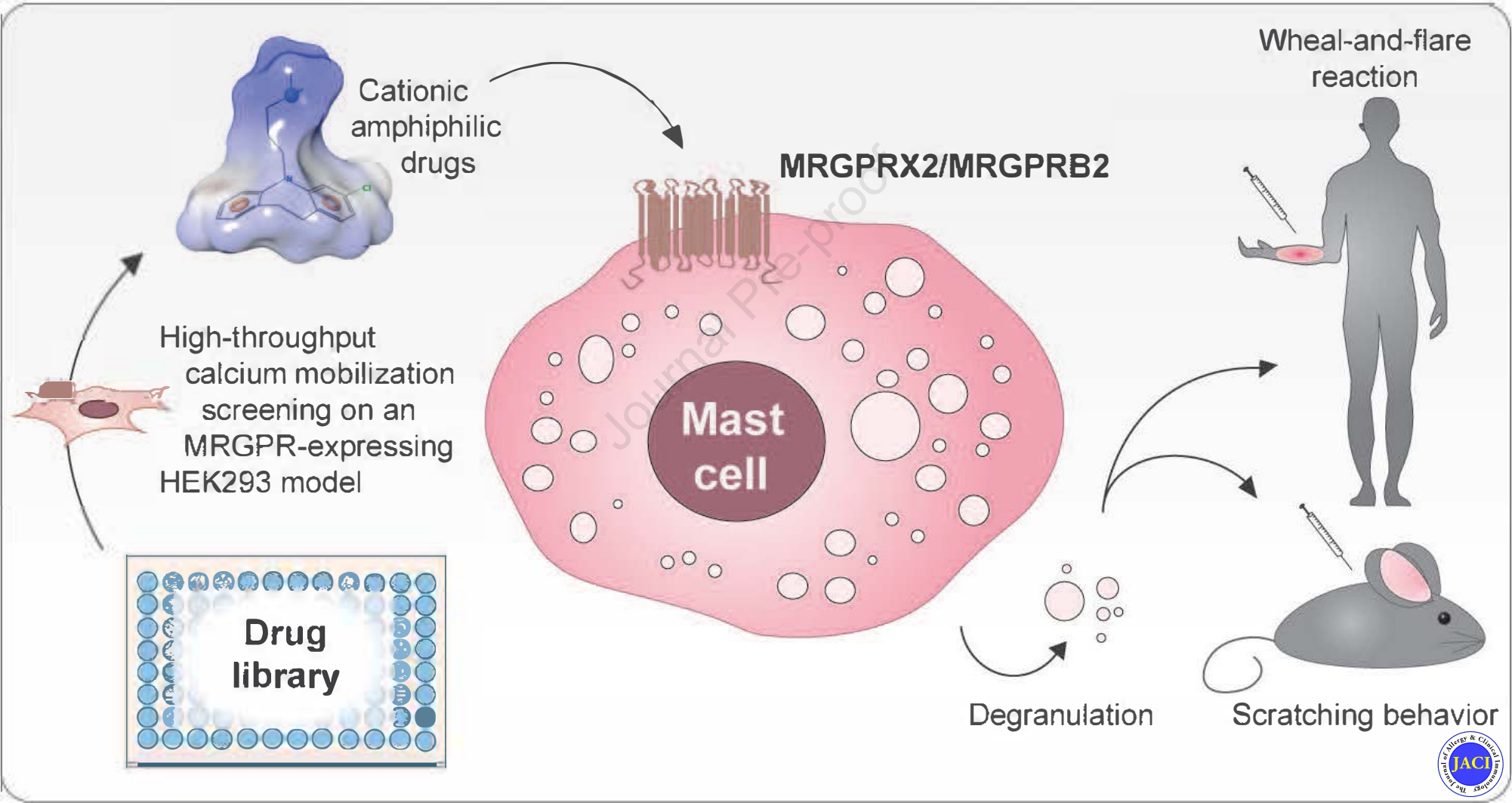

A Group of Cationic Amphiphilic Drugs Activates MRGPRX2 and Induces Scratching Behavior in Mice

Katharina Wolf, PhD#*[a], Helen Kühn, PhD#[a], Felicitas Boehm, MSc[a], Lisa Gebhardt, MSc[a], Markus Glaudo, MSc[a], Konstantin Agelopoulos, PhD[b], Sonja Ständer, MD[b], Philipp Ectors, PhD[c], Dirk Zahn, PhD[c], Yvonne K. Riedel, MSc[d], Dominik Thimm, PhD[d], Christa E. Müller, PhD[d], Sascha Kretschmann, PhD[e], Anita N. Kremer, MD, PhD[e], Daphne Chien[f], BSc, Nathachit Limjunyawong[f], PhD, Qi Peng[f], Xinzhong Dong, PhD[f], Pavel Kolkhir, MD[g,h], Jörg Scheffel, PhD[h], Mia Lykke Søgaard, MSc[a], Benno Weigmann, PhD[a], Markus F. Neurath, MD[a,i], Tomasz Hawro, MD, PhD[h], Martin Metz, MD[h], Michael J.M. Fischer, MD[j], Andreas E. Kremer, MD, PhD*[a]

[a] *Department of Medicine 1, Friedrich-Alexander-University Erlangen-Nürnberg, Germany*

[b] *Center for Chronic Pruritus, Department of Dermatology, University of Münster, Germany*

[c] *Computer Chemistry Center, Friedrich-Alexander-University Erlangen-Nürnberg, Germany (PE now at Roche)*

[d] *PharmaCenter Bonn, Pharmaceutical Institute, Pharmaceutical & Medicinal Chemistry, University of Bonn, Germany*

[e] *Department of Medicine 5, Friedrich-Alexander-University Erlangen-Nürnberg, Germany*

[f] *Solomon H. Snyder Department of Neuroscience, The Johns Hopkins University School of Medicine, Baltimore, USA*

[g] *I.M. Sechenov First Moscow State Medical University (Sechenov University), Division of Immune-mediated skin diseases, Moscow, Russian Federation*

[h] *Dermatological Allergology, Allergie-Centrum-Charité, Department of Dermatology and Allergology, Charité – Universitätsmedizin Berlin, corporate member of Freie Universität Berlin, Humboldt-Universität zu Berlin, and Berlin Institute of Health, Berlin, Germany*

[i] *German Center for Immunotherapy - Deutsches Zentrum Immuntherapie (DZI), Erlangen, Germany*

[j] *Center for Physiology and Pharmacology, University of Vienna, Austria*

#contributed equally

*corresponding authors:

Dr. Katharina Wolf
Department of Medicine 1 (TRC)
University Hospital Erlangen
Schwabachanlage 12
91054 Erlangen
Phone: +49-9131-85 39 602
Email: katharina.b.wolf@fau.de

PD Andreas E. Kremer, MD, PhD, MHBA
Department of Medicine 1
University Hospital Erlangen
Ulmenweg 18
91054 Erlangen
Phone: +49-9131-85 35 000
Email: andreas.kremer@uk-erlangen.de

FUNDING

This article was financially supported by a grant from the German Research Foundation to KA (AG 271/1-1, FOR2690), SST (STA 1159/4-1, FOR2690) and AEK (KR3618/3-1, FOR2690). Additional funding was provided by the interdisciplinary center for clinical research (IZKF) at the Friedrich-Alexander-University of Erlangen-Nürnberg within grant E20 to AEK and within grant E27 to AEK and MJMF. PK was supported by the "Russian Academic Excellence Project 5-100" and a GA²LEN fellowship. KW was supported by a "Bavarian Equal Opportunities Sponsorship" (Realisierung von Chancengleichheit von Frauen in Forschung und Lehre (FFL) – Realization Equal Opportunities for Women in Research and Teaching). CEM is grateful for support by the DFG for the International Research Training Group GRK1873 dedicated to research on G protein-coupled receptors.

AUTHOR CONTRIBUTIONS

KW, HK, FB and AEK designed the study. KW, HK, FB, LG, MG, KA, YKR, SK, DC, NL, QP, PK, MLS, TH acquired data. KW, HK, FB, LG, KA, SST, PE, DZ, YKR, DT, CEM, ANK, XD, PK, JS, BW, MFN, MM, MJMF and AEK analyzed or interpreted data. KW drafted the manuscript with the help of HK and AEK. KW, HK, FB, LG, MG, KA, SST, PE, DZ, YKR, DT, CEM, SK, ANK, DC, NL, QP, XD, PK, JS, MLS, BW, MFN, TH, MM, MJMF and AEK critically revised and finally approved the manuscript.

DISCLOSURE OF POTENTIAL CONFLICT OF INTEREST

Katharina Wolf: no conflicts of interest regarding any aspects of this study.

Helen Kühn: no conflicts of interest regarding any aspects of this study.

Felicitas Boehm: no conflicts of interest regarding any aspects of this study.

Lisa Gebhardt: no conflicts of interest regarding any aspects of this study.

Markus Glaudo: no conflicts of interest regarding any aspects of this study.

Konstantin Agelopoulos: no conflicts of interest regarding any aspects of this study.

Sonja Ständer: SS is advisor of Dermasence, Galderma, Kiniksa Pharmaceuticals, Menlo Therapeutics, Trevi Therapeutics, Novartis, Sanofi, and Vanda Pharmaceuticals Inc, Almirall, Bayer, Beiersdorf, Bellus Health, Bionorica, Cara Therapeutics, Celgene, Clexio Biosciences, DS Biopharma, Galderma, Menlo Therapeutics, Novartis, Perrigo, and Trevi Therapeutics.

Philipp Ectors: no conflicts of interest regarding any aspects of this study.

Dirk Zahn: no conflicts of interest regarding any aspects of this study.

Yvonne K. Riedel: no conflicts of interest regarding any aspects of this study.

Dominik Thimm: no conflicts of interest regarding any aspects of this study.

Christa E. Müller: no conflicts of interest regarding any aspects of this study.

Sascha Kretschmann: no conflicts of interest regarding any aspects of this study.

Anita N. Kremer: no conflicts of interest regarding any aspects of this study.

Daphne Chien: no conflicts of interest regarding any aspects of this study.

Nathachit Limjunyawong: no conflicts of interest regarding any aspects of this study.

Qi Peng: no conflicts of interest regarding any aspects of this study.

Xinzhong Dong: XD is a founder and a scientific advisor of Escient Pharmaceuticals.

Pavel Kolkhir: no conflicts of interest regarding any aspects of this study.

Jörg Scheffel: no conflicts of interest regarding any aspects of this study.

Mia Lykke Søgaard: no conflicts of interest regarding any aspects of this study.

Benno Weigmann: no conflicts of interest regarding any aspects of this study.

Markus F. Neurath: MFN is an advisor of Pentax, PPM, Takeda, Roche, Janssen, Boehringer Ingelheim.

Tomasz Hawro: no conflicts of interest regarding any aspects of this study.

Martin Metz: no conflicts of interest regarding any aspects of this study.

Michael J.M. Fischer: no conflicts of interest regarding any aspects of this study.

Andreas E. Kremer: AEK is a scientific advisor of Escient Pharmaceuticals.

ABSTRACT

Background: Mas gene-related G protein-coupled receptors (MRGPRs) are a GPCR family responsive to various exogenous and endogenous agonists, playing a fundamental role in pain and itch sensation. The primate-specific family member MRGPRX2 and its murine orthologue MRGPRB2 are expressed by mast cells, mediating IgE-independent signaling and pseudo-allergic drug reactions.

Objectives: Therefore, knowledge about the function and regulation of MRGPRX2/MRGPRB2 is of major importance in prevention of drug hypersensitivity reactions and drug-induced pruritus.

Methods: To identify novel MRGPR (ant)agonists, we screened a library of pharmacologically active compounds utilizing a high-throughput calcium mobilization assay. Identified hit compounds were analyzed for their pseudo-allergic and pruritogenic effects in mice and human.

Results: We found a class of commonly used drugs activating MRGPRX2 which consists to a large extent of antidepressants, antiallergic drugs, and antipsychotics. Three-dimensional pharmacophore modeling revealed structural similarities of the identified agonists, classifying them as cationic amphiphilic drugs. Mast cell activation was investigated using the three representatively selected antidepressants clomipramine, paroxetine, and desipramine. Indeed, we could show a concentration-dependent activation and MRGPRX2-dependent degranulation of the human mast cell line LAD2. Furthermore, clomipramine, paroxetine, and desipramine were able to induce degranulation of human skin and murine peritoneal mast cells. These substances elicited dose-dependent scratching behavior upon intradermal injection in C57BL/6 mice but less in MRGPRB2-mutant mice as well as wheal-and-flare reactions upon intradermal injections in humans.

Conclusion: Our results contribute to the characterization of structure-activity relationships and functionality of MRGPRX2 ligands and facilitate prediction of adverse reactions like drug-induced pruritus to prevent severe drug hypersensitivity reactions.

WORD COUNT: 7340 (not including the abstract, figure legends, and references)

NUMBER OF FIGURES/TABLES: 6/1 (+Supplement: 4/2)

KEY MESSAGES:

- A group of commonly used, cationic amphiphilic drugs act as agonists for MRGPRX2, MRGPRB2, and/or MRGPRA1.
- Clomipramine, paroxetine, and desipramine trigger mast cell degranulation causing scratching behavior in mice and wheal-and-flare reactions in humans.
- The structure-activity relationships of MRGPRX2 ligands can help to explain adverse drug reactions as well as drug-induced pruritus and guide development of preventive compounds.

CAPSULE SUMMARY: This study revealed an activation of MRGPRX2 by several cationic amphiphilic drugs which activate mast cells and act as effective pruritogens.

KEY WORDS: Mas gene-related G protein-coupled receptors, mast cells, pseudo-allergic drug reactions, (drug-induced) pruritus

131 **ABBREVIATIONS**

ANOVA – analysis of variants
ATP – adenosine triphosphate
AUC – area under the curve
Bam8-22 – bovine adrenal medulla peptide
BSA – bovine serum albumin
C48/80 – compound 48/80
CHO – chinese hamster ovarian cells
CQ – chloroquine
CST – cortistatin
DAT – dopamine transporter
DC – deoxycholic acid
DHR – drug hypersensitivity reaction
DMEM – Dulbecco's modified eagle medium
DMSO – dimethylsulfoxide
DNA – desoxyribonucleic acid
(D)PBS – Dulbecco's phosphate buffered saline
DRG – dorsal root ganglion
EC_{50} – half maximum effective concentration
FBS – fetal bovine serum
FcεR – receptor for the Fc region of immunoglobulin E
FI – fluorescence intensity
FIASMA – functional inhibitor of acidic sphingomyelinase
FW – forward primer
GFP/YFP – green/yellow fluorescent protein
GPCR – G protein-coupled receptor
HBSS – Hank's balanced salt solution
HEK293 – human embryonic kidney cells
HEPES - 4-(2-hydroxyethyl)-1-piperazineethanesulfonic acid
HPRT – hypoxanthine-guanine phosphoryltransferase
hsMCs – human skin mast cells
i.d., i.p., i.v. – intradermal, intraperitoneal, intravenous
IL – interleukin
LAD2 – Laboratory of Allergic Diseases – 2
LOPAC – library of pharmacologically active compounds
LPA – lysophosphatidic acid
MACS – magnetic cell separation
MOCK – empty vector control
MRGPRs – mas gene-related G protein-coupled receptors
NET – norepinephrine transporter
NPFF – neuropeptide FF
PI – propidium iodide
PIPES – piperazine-N,N′-bis(2-ethanesulfonic acid)
(q)PCR – (quantitative real-time) polymerase chain reaction
mpMCs –murine peritoneal mast cells
pNAG – poly-N-acetylglucosamine
RNA – ribonucleic acid
RPMI – Roswell Park Memorial Institute 1640 medium
RV – reverse primer
SCF – stem cell factor
SEM – standard error of the mean
SERT – serotonin transporter
SIF – simulated intestinal fluid
SP – substance P
SSRI – selective serotonin reuptake inhibitor

TCA – tricyclic antidepressant
TRP – transient receptor potential
VAS – visual analogue scale
WT – wild-type

132

INTRODUCTION

Drug hypersensitivity reactions (DHRs) are undesired events during therapeutic interventions and occur in about 8–15% of all adverse drug reactions.[1] Besides T cell-mediated DHRs, mast cells are key players in most cases, either activated by IgE-dependent, also named "allergic", or IgE-independent, also known as "pseudo-allergic", mechanisms.[2,3,4,5] Both mechanisms provoke mast cell degranulation with release of their granular content including histamine and other biogenic amines, cytokines, proteases, lysosomal enzymes, leukotrienes and prostaglandins. These factors induce smooth muscle contraction, vasodilatation, inflammation and neurotransmission to trigger host defense responses. In case of allergic or pseudo-allergic reactions, they can also trigger edema, urticaria, and pruritus and even a life-threatening anaphylactic shock.[6–8]

Mediating IgE-independent activation of mast cells, the MRGPRX2 (mas gene-related G protein-coupled receptor X2, also known as MRGX2) plays an important role in pseudo-allergic drug reactions.[9–12] In 2001, Dong et al*.* identified a family of GPCRs expressed on sensory neurons with about 50 murine *Mrgprs*, 27 of them have an intact open reading frame (class A–C with several sub-receptors, D, E, F, G), and eight human *MRGPRs* (X1–X4, D, E, F, G).[13] Since then, ongoing research showed an activation of MRGPRs by various structurally diverse substances. Screening of potential MRGPR ligands revealed murine and human receptors with a functional homology: The small peptide bovine adrenal medulla (Bam) 8-22 activates human MRGPRX1 as well as murine MRGPRC11.[14] Chloroquine (CQ) also activates human MRGPRX1 but MRGPRA3 instead of MRGPRC11.[15] Compound 48/80 (C48/80), a polymer produced by condensation of N-methyl-*p*-methoxyphenethylamine with formaldehyde,[16] activates human MRGPRX2 and MRGPRX1 as well as murine MRGPRB2 while the neuropeptide FF (NPFF) can activate both human MRGPRX2 and murine MRGPRA1.[13,17] The biogenic amine β-alanine can induce signaling of human MRGPRD as well as of murine MRGPRD.[18] These findings imply that the primate-specific MRGPR

subfamily X is closely linked to the murine subfamilies A, B, and C, whereas subfamilies D, E, F, and G are concordant between species, based on sequence homology.[19,20]

Members of the MRGPR family, which are expressed on sensory neurons, are not only involved in nociception but also in itch signaling: MRGPRX1 and MRGPRA3 mediate chloroquine-induced pruritus.[15] Chloroquine is a drug used to treat malaria for which severe pruritus as adverse effect was reported, particularly in Africans.[21] Besides chloroquine, several antibiotics, opioids or cytostatic drugs and less commonly selective serotonin reuptake inhibitors (SSRI) and tricyclic antidepressants (TCA) provoke pruritus as an adverse event. The pathway by which these drugs elicit itch is still not fully understood, ranging from acute pruritus by DHRs to chronic pruritus via liver damage.[22] In most cases of itch sensation, exogenous or endogenous pruritogens excite sensory nerve fibers which transmit electrophysiological signals through the spinal cord to the brain. In the central nervous system, signals are processed and eventually transferred to motor neurons inducing a scratch movement.[23,24] Itch signaling starts at the dermal level where pruritogens bind to GPCRs located in the cellular membrane of nerve endings. Activation of these GPCRs can induce a rise of cytosolic calcium levels via the inositol phospholipid signaling pathway which in turn sensitizes and opens depolarizing ion channels such as transient receptor potential (TRP) channels. Depolarization of the neuronal membrane can trigger further voltage-gated ion channels and transforms the stimulus into action potential firing and transmission to the brain.[25,26] The first known pruritogen was histamine, which binds to histamine receptors H1, H2, H3 or H4 and signals via mechanically insensitive C-fibers.[27,28] In contrast, the initial GPCR in non-histaminergic itch, which is mostly transduced by polymodal C-fibers, was unknown until MRGPRs were discovered.[24,29]

MRGPRX2 takes a unique role among MRGPRs as it is expressed in human skin mast cells,[9,30] while its expression on dorsal root ganglion (DRG) neurons is still under debate.[31–33] Immunohistochemistry and quantitative polymerase chain reaction (qPCR) as well as in situ

188 hybridization gave evidence for an MRGPRX2 expression in human DRGs,[32,33] but RNA-Seq
189 analysis of human DRGs did not show a relevant MRGPRX2 expression.[31] Assuming its
190 expression on DRG neurons, MRGPRX2 ligands might induce non-histaminergic itch by
191 direct neuronal activation. Besides, MRGPRX2 causes indirectly histaminergic itch by
192 degranulation of mast cells, thereby releasing histamine which can activate sensory neurons
193 located in the epidermis. MRGPRX2 ligands are structurally diverse exogenous and
194 endogenous compounds, e.g., neuropeptides (i.a. substance P),[34] proteases,[35] antimicrobial
195 peptides,[36,37] opioids[38] and basic secretagogues.[17] Some of these ligands are associated with
196 mast cell activation and MRGPRX2-dependent pseudo-allergic drug reactions.[17,39–41]
197
198 Here, we report on a high-throughput screening on MRGPRs using a library of
199 pharmacologically active compounds. With this approach, we aimed at elucidating molecular
200 traits that lead to the activation or inhibition of these GPCRs. We were interested in i) the
201 “deorphanization” of MRGPRX3 and MRGPRE–G, ii) the activation of MRGPRX2 leading to
202 candidates inducing DHRs including pruritus, and iii) MRGPR inhibitors as potential
203 therapeutics. In this article, we will report on novel MRGPRX2 agonists as potential
204 candidates for DHR.
205

MATERIALS AND METHODS

Human material and subjects

The generation and use of human material for the isolation of primary human cells was approved by the local Charité Ethics Committee, Charité—Universitätsmedizin Berlin Germany (EA1/141/12). Clomipramine was intradermally injected in the volar forearm of five subjects (physicians, coauthors of this publication).

Animals

The C57BL/6 mice (Charles River, Wilmington, MA, USA) were bred in-house in group cages in a temperature-controlled environment on a 12 h light-dark cycle. Food and water were provided ad libitum. The mice were killed aged 6 to 16 weeks in a rising CO_2 atmosphere and by cervical dislocation. Animals from both sexes were used for experiments. All animal experiments conform to the Directive 2010/63/EU and were authorized by the district government (Regierung Unterfranken, Würzburg Ansbach, Germany; reference number 55.2-2532-2-844). For generation of peritoneal mast cell cultures (mpMCs), C57BL/6J mice were obtained from breeding colonies of the animal facilities of Charité - Universitätsmedizin Berlin. Animal care was conducted in accordance with current Institutional Animal Care and Use Committee guidelines at the Charité-Universitätsmedizin Berlin under official permissions of the State of Berlin, Germany. Animal care and experiments for MRGPRB2-mutant mice were conducted in accordance with current Institutional Animal Care and Use Committee guidelines at Johns Hopkins University School of Medicine with approved protocol MO19M34.

Cell lines

Human embryonal kidney (HEK293 and HEK293T) cells were received from American Type Culture Collection (ATCC, Manassas, VA, USA) and cultivated in DMEM (Life Technologies/Thermo Fisher Scientific, Waltham, MA, USA) supplemented with 10% fetal bovine serum (FBS) and 1% penicillin/streptomycin (Pen/Strep). The human mast cell line

234 "Laboratory of Allergic Diseases - 2" (LAD2) was obtained from Dr. Arnold Kirshenbaum and
235 Dr. Dean Metcalfe (National Institute of Allergy and Infectious Diseases (NIAID), NIH,
236 Bethesda, MD, USA) and MRGPRX2-deficient LAD2 cells were generated using
237 CRISPR/Cas9 as described by Shtessel et al.[42,43] Cells were cultured in StemPro-34 SFM
238 (Life Technologies) with nutrient supplements, 1% glutamine, 1% Pen/Strep and 100 ng/mL
239 of human stem cell factor (SCF, Peprotech, Rocky Hill, NJ, USA). Phoenix-A cells were
240 cultivated in RPMI 1640 (Life Technologies) supplemented with 50 µM β-mercaptoethanol
241 (Thermo Scientific), 10% FBS, 2 mM L-glutamine (Life Technologies), 1% minimal essential
242 medium (PAN-Biotech GmbH, Aidenbach, Germany), 1 mM sodium pyruvate (PAN-Biotech)
243 and 40 U/mL Pen/Strep. Cells were tested for mycoplasma every four to eight weeks.
244 Generation and cultivation of primary cells are described in separate paragraphs in the
245 following.
246
247 *Isolation and culture of human skin mast cells*
248 Primary human skin mast cells (hsMCs) were prepared and cultured as described before.[44]
249 Samples from three different donors were cultured and analyzed separately. Purity of MC
250 cultures was routinely checked by flow cytometry for CD117/FcεRI positive cells and was
251 found to be >95%. For detailed description of the isolation procedure see *Materials and*
252 *Methods* in the Online Repository.
253
254 *Isolation and culture of murine peritoneal mast cells*
255 C57BL/6J mice were sacrificed by cervical dislocation and the peritoneal cavity was flushed
256 twice with 5 mL of ice cold DPBS. Cells were collected by centrifugation at 300 g for 3 min
257 and resuspended in RPMI 1640 (Biochrom) supplemented with 25 mM HEPES, 1% non-
258 essential amino acids, 1% Pen/Strep, 10% FBS (all Life Technologies) and 20 ng/mL each
259 recombinant mouse IL-3 and SCF (both Peprotech). Suspension cells were cultured at
260 1.0×10^6 cells/mL with complete media and culture flask change once a week. Purity of

murine peritoneal mast cell (mpMC) cultures were routinely checked by flow cytometry for CD117/FcεRI positive cells and was found to be >95% after 4 weeks in culture.

Isolation and culture of murine DRGs

Adult C57BL/6J mice of both sexes were used to obtain sensory neurons. About 12–20 dorsal root ganglia (DRGs) were harvested from all spinal levels. The procedure was described previously.[45] The nerve roots were removed and the DRGs were incubated in 0.5% streptomyces proteinase, 1% clostridium collagenase (both Sigma-Aldrich) at 37 °C and 5% CO_2 for 30 min. After subsequent mechanical dissociation, the cells were seeded on glass cover slips coated with poly-D-lysine (200 µg/mL, Sigma-Aldrich) and incubated in serum-free TNB 100 medium supplemented with TNB 100 protein-lipid complex (Biochrom), Pen/Strep (100 U/mL each, Life Technologies) and nerve growth factor (mouse NGF 2.5S, 100 ng/mL; Alomone Labs, Tel Aviv, Israel) at 37 °C in a 5% CO_2 atmosphere for 24–30 h before conduction of calcium microfluorimetry experiments.

Cloning of human MRGPRs and murine Mrgprs

The one-exon genes for human *MRGPRX1*, *-X4*, *-D* and *-G* were amplified from human genomic DNA while *MRGPRX2*, *-X3*, *-E* and *-F* were amplified from HeLa cDNA using the PWO Superyield DNA Polymerase Kit (Roche, Basel, Switzerland) following manufacturer's instructions. Human *MRGPRs* were cloned into the pMP71 plasmid containing an IRES followed by green fluorescent protein (GFP), allowing detection of transduced cells.[46,47] The single exon genes for murine *Mrgpra1*, *-a3* and *-b2* were amplified from murine genomic DNA using Phusion High Fidelity DNA Polymerase (Thermo Fisher Scientific). Murine *Mrgprs* were cloned into the mYFP (yellow fluorescent protein)-fusion plasmid producing MRGPR-YFP fusion proteins. For a detailed description of the cloning procedure see *Materials and Methods* in the Online Repository. Inserts were confirmed using Sanger sequencing and subsequent analysis with FinchTV (version 1.4.0, Geospiza, Inc.; Seattle, USA) and Multiple Alignment Construction & Analysis Workbench (MACAW, version 2.0.5).[48]

289

290 *Retroviral constructs and transduction*

291 Phoenix-A cells were transfected as previously described with M57 and pMP71-*MRGPR*
292 plasmids using FuGENE® HD Transfection Reagent (Promega, Madison, WI, USA).[47] After
293 48 h, viral supernatant was collected and used to transduce HEK293 cells on culture plates
294 coated with 30 µg/mL recombinant human retronectin (Takara Bio, Kasatsu, Japan). After
295 approximately one week, transduced cells were sorted for GFP expression by flow cytometry
296 based cell sorting using the FACSAria II (Becton, Dickinson and Company, Franklin Lakes,
297 NJ, USA).

298

299 *Transfection*

300 HEK293T were transiently transfected with murine *Mrgpra1*, *Mrgpra3* or *Mrgprb2* using
301 Lipofectamine 2000 (Invitrogen/ Thermo Fisher Scientific). Therefore, coverslips (Ø22 mm,
302 Thermo Fisher Scientific) were coated with poly-L-lysine (Sigma-Aldrich) for 1 h at room
303 temperature to facilitate cell attachment. After washing the coverslips with DPBS, $1x10^5$ cells
304 per well were seeded in DMEM with 10% FBS and 1% Pen/Strep and placed at 37 °C and
305 5% CO_2 for 24 to 48 h. On the day of transfection, medium was removed and replaced by
306 Opti-MEM (Thermo Fisher Scientific) supplemented with 5% FBS and transfection was
307 conducted following manufacturer's instructions. As all plasmids co-expressed YFP, success
308 of transfection was assessed by fluorescence microscopy using the AMG Evos fluorescence
309 microscope (Thermo Fisher Scientific). Transfected cells were used for further experiments
310 24 – 48 h post transfection. Overexpression of the transfected *Mrgprs* was verified using a
311 PCR.

312

313 *Quantitative real-time PCR*

314 To confirm the successful transduction of HEK293 cells or transfection of HEK293T cells, a
315 qPCR was conducted. RNA from transduced or transfected HEK293 or HEK293T cells was
316 isolated with TriZol (Thermo Fisher Scientific) following the manufacturer's instructions. The

RNA was quantified using a Nanodrop ND1000 Spectrophotometer (Thermo Fisher Scientific). Thereafter, 1 µg of total RNA was translated to cDNA using QuantiNova Reverse Transcription Kit (Qiagen). qPCR was then conducted using SensiFast™ Sybr® No-ROX Kit (Bioline, London, UK), amplifying the cDNA at an annealing temperature of 60 °C for 40 cycles in a CFX Connect qPCR System (Bio-Rad Laboratories). Primer sequences are listed in supplementary table 2 in the Online Repository. Quantification cycles (Cq) were normalized to Cq values of the housekeeping gene hypoxanthin-guanin-phosphoribosyltransferase (HPRT) using the $2^{-\Delta\Delta CT}$ method. For visualization, amplification products were loaded onto a 2% agarose gel supplemented with Midori Green Advanced (Nippon Genetics Europe) and separated for 35 min at 90 V before visualization using a Gel Doc™ XR+ Gel Documentation System (Bio-Rad Laboratories).

Multi-cell fluorometric measurement of cytosolic calcium levels

To investigate activation of all eight human MRGPRs, transduced HEK293 cells were pooled in equal parts immediately before performance of high-throughput experiments. Of the library of pharmaceutically active compounds LOPAC®^{1280} (Sigma-Aldrich/Merck KGaA, Darmstadt, Germany), 720 compounds were used for (ant)agonist screening. Compounds (10 mM in dimethyl sulfoxide (DMSO)) were diluted in DPBS without Ca^{2+} and Mg^{2+} to a final concentration of 30 µM. Compounds, which were positive in the high-throughput calcium mobilization screening, were tested on each MRGPR expressing cell line separately using empty vector cells as control to determine receptor specificity. Therefore, positive agonists were reordered from Sigma-Aldrich in single vials; paroxetine was additionally ordered from Biorbyt (Cambridge, UK). For each experiment, MRGPR-specific positive controls were applied to the cells to test vitality and responsiveness before measuring compounds of interest: Bam8-22 (1 µM; Genemed Synthesis Inc., San Antonio, TX, USA), deoxycholic acid (DC, 100 µM; Sigma-Aldrich) and C48/80 (10 µg/mL, Sigma-Aldrich) diluted in DPBS (without Ca^{2+} and Mg^{2+}). General activation was tested with lysophosphatidic acid 18:1 (LPA, 50 µM; Avanti Polar Lipids, Alabaster, AL, USA). To research inhibitory effects of pharmaceutically

active compounds, the cell pool was stimulated with the library compound to detect activation. After 55 s, the cell pool was treated with the known MRGPRX1 agonist BAM8-22 or known MRGPRX2 agonist C48/80 to examine whether addition of the pharmaceutically active compound caused a reduced rise of cytosolic calcium levels and hence an alleviated activation of MRGPRX1 or MRGPRX2. For a detailed description of multi-cell fluorometric measurement of cytosolic calcium levels see *Materials and Methods* in the Online Repository.

Calcium microfluorimetry of single cells

Calcium microfluorimetry of single cells was used for heterogeneous cell cultures like transiently transfected cells or primary cell cultures with different cell types (e.g., DRG derived cells) as it enables specific detection of cells of interest via imaging. Those cells of interest might be characterized by YFP expression or signaling upon stimulus with a positive control, depending on the experimental setup. For calcium imaging, primary mast or neuronal cells as well as transfected HEK293T cells were stained with the fluorescent calcium indicator dye Fura-2-AM and were measured as described previously.[45,49] For a detailed description of calcium microfluorimetry see *Materials and Methods* in the Online Repository.

PathHunter β-arrestin recruitment assay

A Chinese hamster ovary (CHO) cell line stably expressing β-arrestin, fused to an N-terminal deletion mutant of β-galactosidase, and MRGPRX2 C-terminally tagged with a β-galactosidase fragment (ProLink™) was purchased from DiscoverX (Fremont, CA, USA). Cells were grown in F-12 Ham´s Nutrient Mixture (Life Technologies) supplemented with 10% FBS, 1% Pen/Strep (PAN-Biotech), 800 µg/mL gentamicin (PAN-Biotech) and 300 µg/mL hygromycin B (PAN-Biotech) at 37° C and 5% CO_2. On the day before the assay, cells were seeded into 96-well plates (Nunclon Delta surface plates, Thermo Fisher Scientific) at a density of 2.5×10^5 cells/mL per well in 89 µL of Opti-MEM medium (Thermo Fisher Scientific) supplemented with 2% FBS, 1% Pen/Strep, 800 µg/mL gentamicin and 300

373 µg/mL hygromycin B. Compound dilutions were prepared in DMSO. Cortistatin-14 (CST-14,
374 Bioscience, Bristol, UK), which served as a standard agonist, was diluted in DPBS. In agonist
375 assays, 10 µL of compound dilutions (final concentration: 10 µM) or CST-14 (final
376 concentration: 5 µM) were added to each well after adding 1 µL of DPBS to the compound
377 wells and 1 µL of DMSO to the CST-14 wells. Final DMSO concentrations did not exceed 1%
378 (v/v). For determination of baseline luminescence, DPBS containing 1% DMSO in the
379 absence of compound was used. To each well, 50 µL of detection reagent (DiscoverX) was
380 added. After an incubation period of 60 min at room temperature in the dark, chemo
381 luminescence was measured using a Mithras LB 940 plate reader (Berthold Technologies,
382 Bad Wildbad, Germany). Three to four independent experiments were performed, each in
383 duplicates. The luminescence signals were normalized to the signal of the standard agonist.
384
385 *3D pharmacophore modeling*
386 Computer-based analysis of three-dimensional molecular structures considering
387 physicochemical properties was conducted using Maestro Software (V11 for Linux;
388 Schroedinger, New York City, NY, USA) with the OPLS3 force-field. Each structure was
389 optimized to minimum energy before the analyses. The Ligrep module was used to mimic
390 physiological conditions (pH = 7) and to consider tautomers. Pharmacophore alignment
391 showed structures and binding motifs indicating aromaticity, lipo-/hydrophilicity or hydrogen
392 bridging capacities. The 3D pharmocophore model is based on analyzing motif similarities
393 between the substances and overlaying their geometries.
394
395 *β-hexosaminidase release assay*
396 Measurement of β-hexosaminidase release was conducted to detect mast cell degranulation
397 in LAD2 cells, MRGPRX2-deficient LAD2 cells as well as hsMCs and mpMCs. For a detailed
398 description of β-hexosaminidase release assays in those cell lines see *Materials and*
399 *Methods* in the Online Repository.
400

Annexin V/PI staining

To assess potential toxicity of the newly discovered agonists, LAD2 cells were stained for annexin V and propidium iodide (PI) after 30 min of incubation with varying concentrations of clomipramine, paroxetine, and desipramine in DPBS supplemented with 1 g/L glucose. After stimulation, cells were washed twice with DPBS and once with annexin binding buffer (BioLegend, San Diego, CA, USA) before addition of annexin V-Pacific Blue (1 µL, BioLegend) and PI (1 µL, eBioscience, San Diego, CA, USA). After 15 min of incubation, fluorescent staining of the cells was assessed using MACSQuant® Analyzer 16 Flow Cytometer (Miltenyi Biotec). Pacific Blue was excited using V1 channel with a filter for 400–500 nm whereas PI was measured in channel B3 with an excitation at 595–635 nm. Flow cytometry data was analyzed using FlowJo (version 10, Becton Dickinson). Gating was set with unstimulated samples as well as single color stainings. Cells negative for annexin V and PI were considered viable.

Evans Blue extravasation assay (passive cutaneous anaphylaxis)

1% Evans Blue dissolved in DPBS (100 µL) was injected i.v. before anaesthetizing the C57BL/6N mice by i.p. injection of xylazine (120 mg/kg body weight; Rompun® 2%, Bayer AG, Leverkusen, Germany) and ketamine (24 mg/kg body weight; Ketanest® S, Pfizer, New York City, NY, USA). 5 min after the injections, the anesthetized mice were placed under the Leica EZ4W stereomicroscope (Leica, Wetzlar, Germany) and 10 µL of DPBS and C48/80 (100 µg, 20 g/L) or clomipramine (100 µg, 28.5 mM) dissolved in DPBS were injected intradermally into the left and right ear, respectively. After 15 min mice were sacrificed by cervical dislocation and the ears were removed. To extract Evans Blue from the tissue, the ears were dried for 24 h at 50 °C before incubation in formamide for 24 h at 50 °C under light shaking at 300 rounds per minute. The extracted Evans Blue was then quantified assessing absorbance at 600 nm in the NOVOstar microplate reader (BMG Labtech).

Behavioral scratch assay

Behavioral scratch assays were conducted using C57BL/6N and MRGPRB2-mutant mice from both sexes. For unbiased assessment of acute scratching behavior in C57BL/6N mice upon stimulation with clomipramine, paroxetine, and desipramine, a magnet-based recording technology was used as described before by Kremer et al.[50] MRGPRB2-mutant mice and respective wild-type control mice were kindly provided and scratching was recorded by Prof. Xinzhong Dong and coworkers, using a classical, observation-based recording. In both experimental setups, mice were acclimated in their test chambers and injection of the respective compound of interest (clomipramine (100 µg, 5.69 mM), paroxetine (100 µg, 5.34 mM), desipramine (100 µg, 6.60 mM) and C48/80 (100 µg, 2 g/L)) occurred intradermally in the neck of the mice with a total volume of 50 µL. The amount of all compounds injected was 100 µg per mouse in accordance to the literature for C48/80 used in scratch assays.[51,52] Immediately after injection, scratching was assessed for 30 min. For a detailed description of the behavioral scratch assays see *Materials and Methods* in the Online Repository.

Intradermal injection of clomipramine in healthy volunteers

50 µL of 5 mM clomipramine in simulated intestinal fluid (SIF) and SIF as a negative control were injected i.d., in a single-blinded manner, parallel, randomized left vs. right, in the mid of the volar forearm (2 males, 3 females, age 29-51). Itch intensity was assessed on a visual analogue scale (VAS, 0-100 mm) every single minute starting after provocation up to 30 minutes, for the left and for the right forearm as described previously.[53] Blood flow was assessed using laser speckle contrast imaging (Full-field laser perfusion imager-2, Moor Instruments, Axminster, UK) before provocation as well as 3 minutes and 20 minutes after provocation. Wheal and flare size were measured using a ruler at the same time points.

Data analysis

For statistical analysis, GraphPad Prism version 8 (GraphPad Inc. La Jolla, CA, USA) was used. In case data were positively tested for normal distribution (Kolmogorov-Smirnov), a t-

457 Test was conducted for two groups or an ANOVA for more than two groups. In case data
458 were not normally distributed, a Kruskal-Wallis test was applied. Association of parameters
459 was determined by Pearson's product-momentum correlation for parametric data or by
460 Spearman correlation for non-parametric data. Data are presented as mean ± SEM. Results
461 of statistical inference are indicated for p-values as follows: * $p<0.05$, ** $p<0.01$, *** $p<0.001$,
462 **** $p<0.0001$. Hierarchical cluster analysis of the agonists was conducted with the maximum
463 fluorescence intensity ratio (max. FI 340/380 nm) values of the agonists using IBM SPSS
464 Statistics (version 21, IBM, Armonk, NY, USA). Distances were calculated using average
465 group linkage. To draw area proportional Venn diagrams, EulerApe (University of Kent,
466 Canterbury, UK) was employed.[54]

RESULTS

Several cationic amphiphilic drugs are MRGPRX2 agonists in vitro

In an MRGPR-overexpressing HEK293 model, we examined activation and inhibition of MRGPRs by pharmacologically active compounds. Therefore, we established a HEK293 overexpression model via viral transduction, consisting of eight cell lines expressing one MRGPR each (MRGPRX1, MRGPRX2, MRGPRX3, MRGPRX4, MRGPRD, MRGPRE, MRGPRF, MRGPRG) and an empty vector control (MOCK) (see Fig. S1 in the Online Repository). These cells were used for a high-throughput screening of 720 pharmacologically active compounds measuring a transient rise of cytosolic calcium levels upon activation of the respective GPCR. Thereby, we identified 18 new agonists selective for MRGPRX2 with a maximum fluorescence intensity ratio (FI 340/380 nm) above 1.1, namely aminobenztropine, amitriptyline, benztropine, chlorpheniramine, chlorpromazine, chlorprothixene, citalopram, clemastine, clemizole, clomipramine, clozapine, cyclobenzaprine, cyproheptadine, desipramine, diltiazem, fluoxetine, imipramine and paroxetine (alphabetically ordered). The screening was conducted at a concentration of 30 µM of the respective compound. The maximum FI ratio (1.12–1.92 for 340/380 nm) correlated well with the EC_{50} values (8.15 µM – 206 µM) of all nine substances tested (see Fig. S2 in the Online Repository). The known MRGPRX2 agonist C48/80 served as positive control (Fig. 1A). To classify and order the newly discovered agonists, hierarchical cluster analysis by their maximum ratio of calcium-dependent fluorescence via average group linkage was conducted. Clustering suggested four groups with i) strong (clomipramine, cyproheptadine, chlorpromazine), ii) intermediate (benztropine, chlorprothixene, paroxetine, amitriptyline), iii) weak (imipramine, desipramine, clemastine, aminobenztropine) and iv) very weak (chlorpheniramine, clemizole, citalopram, clozapine, fluoxetine, diltiazem, cyclobenzaprine) activation potential (see Fig. S2 in the Online Repository). For further analysis, the following three representative agonists were selected and studied in detail: clomipramine as a representative of strong agonists, paroxetine as a representative of intermediate agonists, and desipramine as a representative of agonists with weak activation potential. These candidates selectively activated

MRGPRX2- but no other MRGPR- or empty vector control-transduced cells at a concentration of 30 µM (Fig. 1B). Also, clomipramine, paroxetine, and desipramine provoked a concentration-dependent activation of MRGPRX2 with a half-maximal effective concentration (EC_{50}) of 15 µM for clomipramine, 34 µM for paroxetine, and 78 µM for desipramine (Fig. 1C). Analyzing the concentration-response on MOCK cells showed an unspecific Ca^{2+} response of HEK293 cells for high concentrations of 500–1000 µM for clomipramine and desipramine, and of 100 µM in case of paroxetine. Next, concentration-dependent activation of MRGPRX2 by clomipramine, paroxetine, and desipramine was evaluated using an MRGPRX2-dependent β-arrestin recruitment assay based on enzyme complementation technology. The determined EC_{50} values were 9.00 µM for clomipramine, 15.8 µM for paroxetine, and 21.6 µM for desipramine (Fig. 1D). This finding might be of relevance since a β-arrestin assay represents a calcium-independent GPCR signaling pathway, which is responsible for receptor internalization, and not all known MRGPRX2 agonists elicit β-arrestin recruitment.[55]

Three-dimensional pharmacophore modeling was conducted in order to evaluate those ligands' spatial structure. We aimed at identifying structural features that are shared by the new agonists and which would allow us to define motifs that are essential for receptor activation. This computer-based analysis of the 3D molecular structures revealed that all agonists identified in our screening (18 out of 18) carry an aliphatic, protonatable, often tertiary amino group and two benzene rings, while 12 out of 18 compounds additionally feature a hydrophobic center connecting these two aromatic rings (Fig. 2). Thus, all MRGPRX2 agonists share a similar amphiphilic surface charge pattern, which is characterized by negative and positive electrostatic potentials ranging from -0.15 V (blue) to 0.15 V (red). This amphiphilic property is characterized by a lipophilic, aromatic, sterically demanding partial structure, besides an aliphatic but highly polar, weakly basic function, which is, at least in part, positively charged at a physiologic pH value of 7.4. Moreover, 10

out of 18 compounds feature a halogen substituent (fluorine or chlorine) on one of the benzene rings, potentially serving as Lewis-acceptor for σ-hole binding.

In addition to a pharmacophore analysis to identify structural commonalities, we screened the literature to survey functional similarities for our newly discovered MRGPRX2 agonists. We thereto focused on their usage as therapeutics and their respective targets. The newly discovered MRGPRX2 agonists are commonly used as antidepressants (7 out of 18), antiallergic agents (4 out of 18), antipsychotics (3 out of 18) or antispasmodics (3 out of 18) (Table I). Furthermore, 12 out of 18 compounds have a high or medium affinity to serotonin (SERT) and/or norepinephrine (NET) transporters acting as serotonin or norepinephrine reuptake inhibitors; only a few compounds are dopamine reuptake inhibitors binding to dopamine transporters (DAT). Additionally, most agonists have anti-serotonergic, anti-histaminergic, and anti-cholinergic effects, some of them also anti-dopaminergic or anti-adrenergic activities. Receptor–ligand binding affinities were taken either from the Psychoactive Drug Sreening Program (PDSP) Database[56] or from references listed in Table I. As the inhibition constant K_i is strongly dependent on the receptor subtype and might differ between publications, we do not provide exact literature values here. Instead, we classified them into three categories: low (o, K_i = 0.2–20 nM), medium (+, K_i = 21–200 nM), and high (++, K_i = 201–2000 nM). During literature research, one remarkable aspect emerged: due to their amphiphilic character, 12 out of 18 compounds were found to be functional inhibitors of acidic sphingomyelinase (FIASMA). Such compounds enter lysosomes, where they become fully protonated at their aliphatic amino moiety because of the low intra-lysosomal pH value. After protonation, it is impossible for them to cross the membrane anymore. Their lipophilic moiety anchors in the cell membrane and the positively charged portion, which points to the lumen, disturbs electrostatic adherence of acidic sphingomyelinase, which leads to its degradation.[57]

Taken together, when we review the structural and functional commonalities, it becomes clear that this novel class of MRGPRX2 agonists only comprises cationic amphiphilic drugs.

A group of cationic amphiphilic drugs activates human mast cells MRGPRX2-dependently

Subsequently, we were interested in the impact this knowledge might have for common therapeutic interventions. It is well known that MRGPRX2 is expressed on mast cells and provokes IgE-independent degranulation; hence, MRGPRX2 agonists are capable of inducing anaphylactic reactions. Consequently, we experimentally studied activation and degranulation in LAD2 cells and hsMCs by measurements of intracellular calcium mobilization and β-hexosaminidase release assays. First, we confirmed activation of LAD2 cells by 30 µM of aminobenztropine, amitriptyline, benztropine, chlorpheniramine, chlorpromazine, chlorprothixene, citalopram, clomipramine, cyproheptadine, desipramine, diltiazem and paroxetine using 10 µg/mL of C48/80 as a positive control (see Fig. S3A in the Online Repository). The comparison of MRGPRX2 activation in both cell lines, LAD2 (cf. Fig. S3A) and MRGPRX2-expressing HEK293 cells (cf. Fig. 1A), revealed a strong correlation (see Fig. S3B in the Online Repository). This correlation validates our MRGPRX2-expressing HEK293 model as it shows calcium mobilization levels akin to those in human LAD2 cells, which express MRGPRX2 endogenously. Then, we investigated the concentration-dependent activation of LAD2 cells by clomipramine, paroxetine, and desipramine to determine EC_{50} values (Fig. 3A), which were 16 µM for clomipramine, 18 µM for paroxetine, and 34 µM for desipramine. Besides calcium mobilization, clomipramine, paroxetine, and desipramine were also able to provoke a degranulation of LAD2 cells in a concentration-dependent manner (Fig. 3B). At a concentration of 15 µM for clomipramine and of 75 µM for paroxetine, degranulation measured by β-hexosaminidase release was significantly increased in LAD2 cells. The maximum concentration tested for each agonist was determined in accordance with a cell toxicity test (Fig. S3C). For this purpose, the indicated concentrations (50 to 400 µM) of the respective MRGPRX2 agonist were applied to LAD2 cells, which were subsequently stained with propidium iodide (PI) and Annexin V and analyzed by flow cytometry. PI and Annexin V can be used for quantification of apoptotic and necrotic cells; thus, we observed cell toxicity effects for stained cells and full viability for unstained cells. For clomipramine, cell toxicity was detected at a concentration higher than

100 µM, whereas paroxetine and desipramine were less toxic with onset of toxicity above 150 µM and 300 µM, respectively, suggesting that the release of granular content at EC_{50} values is not due to cell death. To prove that the LAD2 degranulation is due to MRGPRX2 activation, a β-hexosaminidase assay in LAD2 cells with a MRGPRX2 knockout was conducted (Fig. 3C). The degranulation caused by 50 µM of clomipramine, paroxetine, and desipramine or 10 µg/mL C48/80 was not above vehicle control in cells lacking MRGPRX2 while wild-type LAD2 exhibited a significantly augmented β-hexosaminidase release. Tween20 (2%) induced comparable signals in both cell lines. Moreover, clomipramine and paroxetine were able to significantly induce degranulation of primary human skin mast cells as of a concentration of 38 µM (clomipramine) and of 75 µM (paroxetine), while desipramine induced a weak, not significant degranulation (Fig. 3D). In summary, MRGPRX2 agonists induced MRGPRX2-dependent β-hexosaminidase release in both LAD2 and primary human mast cells.

A group of cationic amphiphilic drugs activates murine and human mast cells and induces scratching behavior

The physiological relevance of cationic amphiphilic drug-induced mast cell activation and degranulation was investigated in mice and humans. First, activation of mpMCs was evaluated and could be confirmed for all three MRGPRX2 agonists by calcium microfluorimetry using substance P (SP) and C48/80 as positive controls (Fig. 4A). Linear correlation analysis of cells responding to one of the newly discovered agonists and cells responding to the positive control SP or C48/80 was conducted to verify that reacting cells are MRGPRX2-expressing mast cells (Fig. 4B). It revealed clear correlation ($r = 0.42–0.72$, all $p<0.0001$) for clomipramine and desipramine with SP and C48/80 and a weak correlation for paroxetine with SP or C48/80 ($r = 0.31–0.34$, $p<0.0001$). Furthermore, degranulation of mpMCs was assessed in vitro upon stimulation with increasing concentrations of clomipramine, paroxetine, and desipramine and showed a significant response as of a concentration of 38 µM for clomipramine, of 75 µM for paroxetine, and of 150 µM for

desipramine (Fig. 4C). Thus, we aimed to corroborate mast cell degranulation in an in vivo model using Evans Blue dye injected into the tail vein of C57BL/6N mice (Fig. 4D). Clomipramine and the positive control C48/80 significantly enhanced extravasation of Evans Blue stained plasma proteins in the ear of the mice indicating local anaphylaxis with an augmented histamine concentration.[58] Next, we utilized the MRGPRX2 orthologue MRGPRB2, expressed on mast cells, which we hypothesized to be also activated by the newly discovered MRGPRX2 agonists. Calcium microfluorimetry on HEK293T cells transfected with either *Mrgprb2* or an empty vector control exhibited activation of *Mrgprb2*-transfected cells by clomipramine, paroxetine, desipramine and the control agonist C48/80 (Fig. 4E+F). For paroxetine, the mean response of pooled MRGPRB2-expressing HEK293T cells showed only a minor elevation of the calcium signal compared to control cells. However, individual *Mrgprb2*-transfected cells showed clear responses to treatment with clomipramine and desipramine.

The human MRGPRX2 is suggested to be not only expressed on mast cells but also on neuronal cells of DRGs.[32,33] Thus, MRGPRX2 agonists may directly activate a neuronal signaling cascade in humans. Since MRGPRB2 is not expressed on murine DRG neurons, but other murine MRGPRs are, we tested their direct activation by our newly discovered agonists. Calcium microfluorimetry of dissociated murine DRG cells evidenced that clomipramine (10–100 µM), paroxetine (25–100 µM), and desipramine (100 µM) were capable to directly activate neuronal cells (see Fig. S4A in the Online Repository). The TRPA1 agonist carvacrol and the TRPV1 agonist capsaicin were applied to the same cells. So, cells responding to clomipramine, paroxetine, and desipramine could be characterized by their TRP expression using area proportional Venn diagrams (see Fig. S4B in the Online Repository). Interestingly, the three agonists mainly activated neurons expressing TRPV1 or both channels but rarely cells expressing only TRPA1. MRGPRA1 and MRGPRA3 are murine MRGPRs expressed on sensory neurons.[13] Thus, clomipramine, paroxetine, and desipramine were tested on HEK293T cells transfected with *Mrgpra1* and *Mrgpra3* or an

empty vector control. All three compounds induced substantial calcium mobilization in around 60–90% of all cells positive for MRGPRA1 (determined by YFP expression), whereas they did not activate MRGPRA3 or control cells (see Fig. S4C in the Online Repository). The neuropeptide FF (NPFF) was used as a positive control for MRGPRA1 and chloroquine for MRGPRA3. Clomipramine, paroxetine, and desipramine induced a minimal signal on empty vector control cells, substantially weaker than in MRGPRA1-expressing cells.

MRGPR receptors are also known as "itch receptors".[59] Thus, we aimed to investigate the pruritogenic potential of the newly discovered MRGPR agonists using a murine scratching model and intradermal injection in the skin of five subjects.[50,53] Indeed, intradermal injection of 100 µg of clomipramine (5.7 mM), paroxetine (5.3 mM), or desipramine (6.6 mM) per site in the neck of C57BL/6N mice induced substantial scratching behavior, detected observer-independently using a magnet-based recording technology (Fig. 5A). C48/80 served as a positive control to induce scratching behavior. Clomipramine and paroxetine elicited substantial scratching of 109±48 and 108±49 scratch bouts, respectively, within 30 min after injection compared to 21±16 scratch bouts after application of PBS. The responsiveness of individual mice suggests also a pruritogenic potential of desipramine, albeit there was no significant difference to PBS control with the pre-specified number of animals and the large variance observed. Furthermore, scratching behavior was induced dose-dependently injecting either 0.1, 1 or 10 mM of clomipramine. At concentrations of 1 mM (18 µg/site) and above, scratch bouts were significantly enhanced within 30 min after injection in comparison to the negative control PBS (Fig. 5B). There was no dependency on the sex of the mice perceived (data not shown). Compared with C57BL/6 wild-type animals, MRGPRB2-mutant animals scratched significantly less in response to injection of clomipramine and desipramine suggesting that MRGPRB2 mediates a component of cationic amphiphilic drug-induced pruritus (Fig. 5C-E). When injecting clomipramine (50 µL, 5 mM) in the skin of the volar forearm of five healthy volunteers (physicians, co-authors), a fast and substantial mast cell activation was observed (Fig. 6). Mast cell activation was determined i) by a wheal-and-flare

662 reaction measured with a ruler at 3 min (data not shown) and 20 min after provocation
663 showing a significantly increased reaction upon provocation with clomipramine in comparison
664 to vehicle control (SIF) and ii) by a significant blood flow change in comparison to baseline
665 using laser speckle contrast imaging at the same time points. Out of five subjects, one
666 subject (#1) reported about a distinct, long-lasting itch sensation upon provocation with
667 clomipramine, one subject (#4) about mild itch, and one subject (#2) about a very subtle,
668 itch-like sensation (Fig. 6E). Taken together, the maximal pruritus intensity was not
669 significantly enhanced upon intradermal injection of clomipramine in comparison to vehicle
670 control (Fig. 6D), albeit a high individual variance was observed with itch induction in some
671 subjects.

DISCUSSION

The GPCR MRGPRX2 is known to play an important role in pseudo-allergic drug reactions.[11] Here, we introduce a novel class of cationic amphiphilic drugs as agonists for this receptor identified by means of a high-throughput calcium mobilization screening. Considering the agonists' molecular structure and activation capacity, we hypothesize the following structural elements to be of major importance for MRGPRX2 activation: i) the aromatic ring system is preferably tricyclic with a hydrophobic center and has a halogen substituent, ii) the aliphatic amino group is tertiary or otherwise sterically demanding and arranged orthogonally to the axis of the ring system. Aromaticity in combination with a protonatable amino group can also be found in opioids, phenothiazines, fluoroquinolone antibiotics and neuromuscular blocking agents, already published as MRGPRX2 agonists, which is in line with our findings. Their EC_{50} values in calcium mobilization assays ranged from 6 µM for opioids to 25 µM for phenothiazines and, thus, are similar to the EC_{50} values of cationic amphiphilic drugs presented here.[17,39,60] All newly characterized agonists target receptors or transporters for monoamine neurotransmitters. Analysis and structural comparison via in silico homology modeling of the well-known sequences of the respective receptors, many of which have been co-crystallized with their ligands, and MRGPRX2 could be performed.[60] To determine structural elements consistent between known agonists and to characterize the MRGPRX2 binding pocket may facilitate the identification of other novel MRGPRX2 agonists and the prevention of DHRs.

Next, we investigated the physiological relevance of the newly discovered MRGPRX2 agonists by using mast cells which express MRGPRX2 or MRGPRB2 endogenously.[61] In the human mast cell line LAD2 as well as in primary human and murine mast cells, calcium mobilization and degranulation were induced by clomipramine, paroxetine, and positive controls and a similar tendency was observed for desipramine.[62,63] In LAD2 cells lacking MRGPRX2, degranulation was decreased to the level of vehicle control implying that MRGPRX2 is crucial for mast cell degranulation upon stimulation with cationic amphiphilic

drugs. In murine mast cells, paroxetine also induced calcium mobilization in cells, which were not MRGPRB2-expressing based on a lack of response to C48/80 (cf. Fig. 4B and 4F). Although there are several studies showing that paroxetine has no affinity to serotonin receptors, recent publications demonstrated that paroxetine and other SSRIs like sertraline, citalopram or fluoxetine, can induce pruritus via 5-HT_{2B} receptors.[64–66] Since mast cells are proposed to express 5-HT_{2B} and other serotonin receptors, paroxetine could signal via several receptors on mast cells, including the here described activation of MRGPRX2.[67] Besides potential activation of other GPCRs, clomipramine and paroxetine provided an indication for inhibition of calcium channels: in calcium microfluorimetry experiments, they lowered the basal calcium level in mast cells before calcium mobilization upon GPCR activation occurred (cf. Fig. 4A).[68,69] Furthermore, HEK293T cells transiently transfected with the murine *Mrgprb2* receptor responded to stimulation with the newly discovered agonists, although not all transfected cells positive for YFP tagged to *Mrgprb2* were activated by C48/80 or clomipramine, paroxetine, and desipramine. Accordingly, small molecule drugs identified as MRGPRX2 activators by McNeil et al. exhibited explicitly different EC_{50} on MRGPRB2, suggesting there is indeed a functional homology between MRGPRX2 and MRGPRB2 but no full analogy.[17] Hence, cationic amphiphilic drugs signal via MRGPRX2 and MRGPRB2 but possibly not exclusively, therefore even GPCR-independent mechanisms might play a role.[70] This hypothesis is conceivable since higher concentrations of clomipramine, paroxetine, and desipramine activated HEK293 cells in a concentration-dependent manner (cf. Fig. 1C). Nevertheless, our data show convincing evidence for an activation of primary human and murine mast cells by the cationic amphiphilic drugs clomipramine, paroxetine, and desipramine.

Activation of mast cells not only triggers inflammatory signaling pathways resulting in enhanced vascular permeability and recruitment of other immune cells,[71] there is also an interaction of mast cells and neuronal cells modulating itch and pain sensation.[72] We investigated the activation of murine DRG neurons by clomipramine, paroxetine, and

desipramine and the respective overlap with cells responding to TRPV1 agonist capsaicin and TRPA1 agonist carvacrol. Histaminergic itch is assumed to signal via TRPV1, while activation of TRPA1 is associated with non-histaminergic, MRGPR-mediated itch.[73] In calcium microfluorimetry, 7-9% of all detected cells reacted to the three new agonists and Venn diagrams depict the overlap of reacting cells with $TRPV1^+$ and $TRPA1^+$ cells. Remarkably, most cells activated by the newly discovered agonists were positive for TRPV1, some additionally expressed TRPA1. Thus, signaling circuits of DRG neurons induced by clomipramine, paroxetine, and desipramine would need further investigation. To identify the responsible murine MRGPRs in DRG neurons, MRGPRA1 and MRGPRA3 were tested as they are expressed on neuronal cells and MRGPRA1 was proposed to be a functional homologue of MRGPRX2.[13,15,74] Cells transfected with *Mrgpra1* were activated by clomipramine, paroxetine, and desipramine. In contrast, clomipramine, paroxetine or desipramine did not elicit responses in HEK293T cells transfected with *Mrgpra3*, while moderate responses to the known MRGPRA3 agonist chloroquine served as positive control for functional expression. Thus, the results propose MRGPRA1 as neuronal MRGPR mediating neuronal responses to the identified cationic amphiphilic drugs. How MRGPRs modulate the interplay between mast cells and neuronal cells and how the organism benefits from expression of MRGPRs on both cell types remains to be elucidated.

Pruritus can be one symptom of (pseudo-)allergic reactions, which is not restricted to the injection site but is processed via the spinal cord and the brain.[75,76] For this reason, we investigated the pruritogenic potential of the newly discovered agonists in vivo. In mice, clomipramine and paroxetine induced scratching behavior, desipramine showed a similar tendency. Thus, our data represent the first evidence for substances with a particular pharmacophore, all of which are clinically used drugs, to be effective pruritogens in mice. Interestingly, itch sensation towards clomipramine in humans was highly individual within the five subjects investigated, which might possibly be caused by MRGPRX2 polymorphisms.[77] Nonetheless, there was a clear mast cell activation in terms of a wheal-and-flare reaction and

a blood flow change detectable in all subjects. However, the impact on the medical treatment of patients with depression and psychotic disorders or allergies remains ambiguous. Antipsychotics and antidepressants in general are assumed to induce miscellaneous dermatological reactions,[78–80] anaphylaxis,[81] and pruritus,[22,82] but also serve for treatment of psychogenic and chronic pruritus.[83–86] Topical application of doxepin, a tricyclic antidepressant with similar structure to clomipramine, desipramine, and imipramine, induced contact dermatitis with eczema and itch sensation.[87,88] Additionally, clomipramine can mediate infrequent but severe cutaneous adverse drug reactions.[89,90] Also antihistamines, commonly used in allergic disorders to relieve mast cell-mediated symptoms,[91] are presumed to be able to lead to an anaphylaxis and hypersensitivity reaction in very rare cases.[81,87,92] However, it should be considered that the observed effects might be a continuation of the initial allergic or anaphylactic event. The immediate and non-immediate adverse reactions of the newly discovered MRGPRX2 agonists shown here could be different for oral and intravenous administration as it is assumed for β-lactam antibiotics.[93,94] Neuromuscular blocking agents, which are known to activate MRGPRX2 and which are mostly administered intravenously, are often associated with drug-induced perioperative hypersensitivity reactions.[95–97] Though, orally administered drugs, like clomipramine, paroxetine, and desipramine, undergo metabolism in gut and liver and their metabolites might exhibit an altered reaction profile than that of the parent drug. At first sight, it may be odd that first-generation H1 antihistamines and antipruritics activate MRGPRX2 on mast cells inducing degranulation with histamine release and scratching behavior in mice. Hou et al. found the antipsychotic chlorpromazine to release histamine from mast cells via MRGPRX2, but at the same time, it inhibited calcium mobilization by histamine receptor H1 in overexpressing HEK293 cells.[39] This allows to formulate the hypothesis, that MRGPRX2 might modulate the histamine-signaling pathway at the interplay of mast cells and neuronal cells.

ACKNOWLEDGEMENTS

The authors thank Selina Drechsler, Katharina Kalb, Victoria Leibl, Freya Wolff and Alina Bauer for excellent technical support as well as Stephan E. Wolf and Felix B. Engel for fruitful discussions.

REFRENCES

1. Böhm R, Proksch E, Schwarz T, Cascorbi I. Drug Hypersensitivity - Diagnosis, Genetics, and Prevention. Dtsch Arztebl Int. 2018;115:501–12.
2. Pichler WJ, Hausmann O. Classification of Drug Hypersensitivity into Allergic, p-i, and Pseudo-Allergic Forms. Int Arch Allergy Immunol. 2017;171:166–79.
3. Spoerl D, Nigolian H, Czarnetzki C, Harr T. Reclassifying anaphylaxis to neuromuscular blocking agents based on the presumed Patho-Mechanism: IgE-Mediated, pharmacological adverse reaction or “innate hypersensitivity”? Int J Mol Sci. 2017;18:1–14.
4. Mayorga C, Fernandez TD, Montañez MI, Moreno E, Torres MJ. Recent developments and highlights in drug hypersensitivity. Allergy Eur J Allergy Clin Immunol. 2019;1–14.
5. Zhang B, Li Q, Shi C, Zhang X. Drug-induced pseudoallergy: A review of the causes and mechanisms. Pharmacology. 2017;101:104–10.
6. Wernersson S, Pejler G. Mast cell secretory granules: Armed for battle. Nat Rev Immunol. 2014;14:478–94.
7. Bulfone-Paus S, Nilsson G, Draber P, Blank U, Levi-Schaffer F. Positive and Negative Signals in Mast Cell Activation. Trends Immunol [Internet]. 2017;38:657–67. Available from: http://dx.doi.org/10.1016/j.it.2017.01.008
8. Finkelman FD, Khodoun M V., Strait R. Human IgE-independent systemic anaphylaxis. J Allergy Clin Immunol [Internet]. 2016;137:1674–80. Available from: http://dx.doi.org/10.1016/j.jaci.2016.02.015
9. Tatemoto K, Nozaki Y, Tsuda R, Konno S, Tomura K, Furuno M, et al. Immunoglobulin E-independent activation of mast cell is mediated by Mrg receptors. Biochem Biophys Res Commun. 2006;349:1322–8.
10. Grimes J, Desai S, Charter NW, Lodge J, Moita Santos R, Isidro-Llobet A, et al. MrgX2 is a promiscuous receptor for basic peptides causing mast cell pseudo-allergic and anaphylactoid reactions. Pharmacol Res Perspect. 2019;7:1–12.

11. Subramanian H, Gupta K, Ali H. Roles of Mas-related G protein–coupled receptor X2 on mast cell–mediated host defense, pseudoallergic drug reactions, and chronic inflammatory diseases. J Allergy Clin Immunol [Internet]. 2016;138:700–10. Available from: http://dx.doi.org/10.1016/j.jaci.2016.04.051
12. Porebski G, Kwiecien K, Pawica M, Kwitniewski M. Mas-Related G Protein-Coupled Receptor-X2 (MRGPRX2) in Drug Hypersensitivity Reactions. Front Immunol. 2018;9:3027.
13. Dong X, Han S kyou, Zylka MJ, Simon MI, Anderson DJ. A diverse family of GPCRs expressed in specific subsets of nociceptive sensory neurons. Cell. 2001;106:619–32.
14. Lembo PMC, Grazzini E, Groblewski T, O'donnell D, Roy MO, Zhang J, et al. Proenkephalin A gene products activate a new family of sensory neuron-specific GPCRs. Nat Neurosci. 2002;5:201–9.
15. Liu Q, Tang Z, Surdenikova L, Kim S, Patel KN, Kim A, et al. Sensory Neuron-Specific GPCR Mrgprs Are Itch Receptors Mediating Chloroquine-Induced Pruritus. Cell [Internet]. 2009;139:1353–65. Available from: http://dx.doi.org/10.1016/j.cell.2009.11.034
16. PATON WD. Compound 48/80: a potent histamine liberator. Br J Pharmacol Chemother. 1951;6:499–508.
17. McNeil BD, Pundir P, Meeker S, Han L, Undem BJ, Kulka M, et al. Identification of a mast-cell-specific receptor crucial for pseudo-allergic drug reactions. Nature [Internet]. 2015;519:237–41. Available from: http://dx.doi.org/10.1038/nature14022
18. Shinohara T, Harada M, Ogi K, Maruyama M, Fujii R, Tanaka H, et al. Identification of a G protein-coupled receptor specifically responsive to β-alanine. J Biol Chem. 2004;279:23559–64.
19. Zylka MJ, Dong X, Southwell AL, Anderson DJ. Atypical expansion in mice of the sensory neuron-specific Mrg G protein-coupled receptor family. Proc Natl Acad Sci U S A. 2003;100:10043–8.
20. Meixiong J, Dong X. Mas-Related G Protein–Coupled Receptors and the Biology of

Itch Sensation. Annu Rev Genet. 2017;51:103–21.

21. Osifo NG. Chloroquine-Induced Pruritus Among Patients With Malaria. Arch Dermatol [Internet]. 1984;120:80. Available from: http://archderm.jamanetwork.com/article.aspx?doi=10.1001/archderm.1984.01650370086015

22. Reich A, Ständer S, Szepietowski JC. Drug-induced pruritus: A review. Acta Derm Venereol. 2009;89:236–44.

23. Yosipovitch G, Bernhard JD. Chronic pruritus. N Engl J Med. 2013;368:1625–34.

24. Dhand A, Aminoff MJ. The neurology of itch. Brain. 2014;137:313–22.

25. Bautista DM, Wilson SR, Hoon MA. Why we scratch an itch: The molecules, cells and circuits of itch. Nat Neurosci [Internet]. 2014;17:175–82. Available from: http://dx.doi.org/10.1038/nn.3619

26. Lay M, Dong X. Neural Mechanisms of Itch. Annu Rev Neurosci. 2020;43:187–205.

27. Simone DA, Ngeow JYF, Whitehouse J, Becerra-Cabal L, Putterman GJ, Lamotte RH. The Magnitude and Duration of Itch Produced by Intracutaneous Injections of Histamine. Somatosens Res [Internet]. 1987;5:81–92. Available from: http://www.tandfonline.com/doi/full/10.3109/07367228709144620

28. Rossbach K, Nassenstein C, Gschwandtner M, Schnell D, Sander K, Seifert R, et al. Histamine H 1, H 3 and H 4 receptors are involved in pruritus. Neuroscience [Internet]. 2011;190:89–102. Available from: http://dx.doi.org/10.1016/j.neuroscience.2011.06.002

29. Dong X, Dong X. Peripheral and Central Mechanisms of Itch. Neuron [Internet]. 2018;98:482–94. Available from: https://doi.org/10.1016/j.neuron.2018.03.023

30. Varricchi G, Pecoraro A, Loffredo S, Poto R, Rivellese F, Genovese A, et al. Heterogeneity of human mast cells with respect to MRGPRX2 receptor expression and function. Front Cell Neurosci. 2019;13:1–10.

31. Flegel C, Schöbel N, Altmüller J, Becker C, Tannapfel A, Hatt H, et al. RNA-Seq analysis of human trigeminal and dorsal root ganglia with a focus on chemoreceptors.

PLoS One. 2015;10:1–30.

32. Robas N, Mead E, Fidock M. MrgX2 Is a High Potency Cortistatin Receptor Expressed in Dorsal Root Ganglion. J Biol Chem. 2003;278:44400–4.

33. Zhang L, Taylor N, Xie Y, Ford R, Johnson J, Paulsen JE, et al. Cloning and expression of MRG receptors in macaque, mouse, and human. Mol Brain Res. 2005;133:187–97.

34. Azimi E, Reddy VB, Pereira PJS, Talbot S, Woolf CJ, Lerner EA. Substance P activates Mas-related G protein–coupled receptors to induce itch. J Allergy Clin Immunol [Internet]. 2017;140:447–453.e3. Available from: http://dx.doi.org/10.1016/j.jaci.2016.12.980

35. Reddy VB, Sun S, Azimi E, Elmariah SB, Dong X, Lerner EA. Redefining the concept of protease-activated receptors: Cathepsin S evokes itch via activation of Mrgprs. Nat Commun. 2015;6:1–10.

36. Subramanian H, Gupta K, Guo Q, Price R, Ali H. Mas-related gene X2 (MrgX2) is a novel G protein-coupled receptor for the antimicrobial peptide LL-37 in human mast cells: resistance to receptor phosphorylation, desensitization, and internalization. J Biol Chem. 2012;

37. Subramanian H, Gupta K, Lee D, Bayir AK, Ahn H, Ali H. β-Defensins Activate Human Mast Cells via Mas-Related Gene X2. J Immunol. 2013;191:345–52.

38. Lansu K, Karpiak J, Liu J, Huang X-P, McCorvy JD, Kroeze WK, et al. In silico design of novel probes for the atypical opioid receptor MRGPRX2. Nat Chem Biol [Internet]. 2017;13:529–36. Available from: http://www.nature.com/articles/nchembio.2334

39. Hou Y, Che D, Wei D, Wang C, Xie Y, Zhang K, et al. Phenothiazine antipsychotics exhibit dual properties in pseudo-allergic reactions: Activating MRGPRX2 and inhibiting the H 1 receptor. Mol Immunol [Internet]. 2019;111:118–27. Available from: https://doi.org/10.1016/j.molimm.2019.04.008

40. Ferry X, Brehin S, Kamel R, Landry Y. G protein-dependent activation of mast cell by peptides and basic secretagogues. Peptides. 2002;23:1507–15.

41. Kühn H, Kolkhir P, Babina M, Düll M, Frischbutter S, Fok JS, et al. Mas-related G protein-coupled receptor X2 and its activators in dermatologic allergies. J Allergy Clin Immunol [Internet]. 2020; Available from: http://www.ncbi.nlm.nih.gov/pubmed/33071069

42. Kirshenbaum AS, Akin C, Wu Y, Rottem M, Goff JP, Beaven MA, et al. Characterization of novel stem cell factor responsive human mast cell lines LAD 1 and 2 established from a patient with mast cell sarcoma/leukemia; activation following aggregation of FcεRI or FcγRI. Leuk Res [Internet]. 2003;27:677–82. Available from: https://linkinghub.elsevier.com/retrieve/pii/S0145212602003430

43. Shtessel M, Limjunyawong N, Oliver ET, Chichester K, Gao L, Dong X, et al. MRGPRX2 Activation Causes Increased Skin Reactivity in Chronic Spontaneous Urticaria Patients. J Invest Dermatol [Internet]. 2020; Available from: https://linkinghub.elsevier.com/retrieve/pii/S0022202X20319618

44. Guhl S, Artuc M, Neou A, Babina M, Zuberbier T. Long-term cultured human skin mast cells are suitable for pharmacological studies of anti-allergic drugs due to high responsiveness to FceRI cross-linking. Biosci Biotechnol Biochem. 2011;75:382–4.

45. Robering JW, Gebhardt L, Wolf K, Kühn H, Kremer AE, Fischer MJM. Lysophosphatidic acid activates satellite glia cells and Schwann cells. Glia. 2019;67:999–1012.

46. Engels B, Cam H, Schüler T, Indraccolo S, Gladow M, Baum C, et al. Retroviral vectors for high-level transgene expression in T lymphocytes. Hum Gene Ther. 2003;14:1155–68.

47. Griffioen M, Van Egmond HME, Barnby-Porritt H, Van Der Hoorn MAWG, Hagedoorn RS, Kester MGD, et al. Genetic engineering of virus-specific T cells with T-cell receptors recognizing minor histocompatibility antigens for clinical application. Haematologica. 2008;93:1535–43.

48. Lawrence CE, Altschul SF, Boguski MS, Liu JS, Neuwald AF, Wootton JC. Detecting subtle sequence signals: A gibbs sampling strategy for multiple alignment. Science.

1993;262:208–14.

49. Dittert I, Vlachová V, Knotková H, Vitásková Z, Vyklicky L, Kress M, et al. A technique for fast application of heated solutions of different composition to cultured neurones. J Neurosci Methods. 1998;82:195–201.

50. Kremer AE, Martens JJWW, Kulik W, Rueff F, Kuiper EMM, Van Buuren HR, et al. Lysophosphatidic acid is a potential mediator of cholestatic pruritus. Gastroenterology [Internet]. 2010;139:1008–1018.e1. Available from: http://dx.doi.org/10.1053/j.gastro.2010.05.009

51. Obara I, Medrano MC, Signoret-Genest J, Jiménez-Díaz L, Géranton SM, Hunt SP. Inhibition of the mammalian target of rapamycin complex 1 signaling pathway reduces itch behaviour in mice. Pain. 2015;156:1519–29.

52. Kühn H, Kappes L, Wolf K, Gebhardt L, Neurath MF, Reeh P, et al. Complementary roles of murine NaV1.7, NaV1.8 and NaV1.9 in acute itch signalling. Sci Rep. 2020;10:1–12.

53. Lehmann S, Deuring E, Weller K, Scheffel J, Metz M, Maurer M, et al. Flare Size but Not Intensity Reflects Histamine-Induced Itch. Skin Pharmacol Physiol [Internet]. 2020;1–9. Available from: https://www.karger.com/Article/FullText/508795

54. Micallef L, Rodgers P. euler APE: Drawing area-proportional 3-Venn diagrams using ellipses. PLoS One. 2014;9.

55. Roy S, Ganguly A, Haque M, Ali H. Angiogenic Host Defense Peptide AG-30/5C and Bradykinin B 2 Receptor Antagonist Icatibant Are G Protein Biased Agonists for MRGPRX2 in Mast Cells . J Immunol. 2019;202:1229–38.

56. Roth B, Drsicol J. Psychoactive Drug Screening Program (PDSP). Univ North Carolina Chapel Hill United States Natl Inst Ment Heal. 2020;retrieved:January 21, 2020.

57. Beckmann N, Sharma D, Gulbins E, Becker KA, Edelmann B. Inhibition of acid sphingomyelinase by tricyclic antidepressants and analogons. Front Physiol. 2014;5 AUG.

58. Evans H, Killoran KE, Mitre E. Measuring local anaphylaxis in mice. J Vis Exp.

2014;1–6.

59. Espino SS, Robinson SD, Safavi-Hemami H, Gajewiak J, Yang W, Olivera BM, et al. Conopeptides promote itch through human itch receptor hMgprX1. Toxicon [Internet]. 2018;154:28–34. Available from: https://linkinghub.elsevier.com/retrieve/pii/S004101011830374X

60. Lansu K, Karpiak J, Liu J, Huang XP, McCorvy JD, Kroeze WK, et al. In silico design of novel probes for the atypical opioid receptor MRGPRX2. Nat Chem Biol. 2017;13:529–36.

61. Subramanian H, Kashem SW, Collington SJ, Qu H, Lambris JD, Ali H. PMX-53 as a dual CD88 antagonist and an agonist for mas-related gene 2 (MrgX2) in human mast cells. Mol Pharmacol. 2011;79:1005–13.

62. Tasaka K, Mio M, Okamoto M. Intracellular calcium release induced by histamine releasers and its inhibition by some antiallergic drugs. Ann Allergy [Internet]. 1986;56:464–9. Available from: http://www.ncbi.nlm.nih.gov/pubmed/2424349

63. Jozaki K, Kuriu A, Waki N, Adachi S, Yamatodani A, Tarui S, et al. Proliferative potential of murine peritoneal mast cells after degranulation induced by compound 48/80, substance P, tetradecanoylphorbol acetate, or calcium ionophore A23187. J Immunol. 1990;145:4252–6.

64. Bourin M, Chue P, Guillon Y. Paroxetine: A review [Internet]. Vol. 7, CNS Drug Reviews. 2001. p. 25–47. Available from: http://doi.wiley.com/10.1111/j.1527-3458.2001.tb00189.x

65. Lee SH, Cho PS, Tonello R, Lee HK, Jang JH, Park GY, et al. Peripheral serotonin receptor 2B and transient receptor potential channel 4 mediate pruritus to serotonergic antidepressants in mice. J Allergy Clin Immunol. 2018;142:1349–1352.e16.

66. Peng L, Gu L, Li B, Hertz L. Fluoxetine and all other SSRIs are 5-HT_{2B} Agonists - Importance for their Therapeutic Effects. Curr Neuropharmacol. 2014;12:365–79.

67. Kushnir-Sukhov NM, Gilfillan AM, Coleman JW, Brown JM, Bruening S, Toth M, et al. 5-Hydroxytryptamine Induces Mast Cell Adhesion and Migration. J Immunol.

2006;177:6422–32.

68. Yaris E, Kesim M, Kadioglu M, Kalyoncu NI, Ulku C, Ozyavuz R. The effects of paroxetine on rat isolated vas deferens. Pharmacol Res. 2003;48:335–45.

69. Mousavizadeh K, Ghafourifar P, Sadeghi-Nejad H. Calcium channel blocking activity of thioridazine, clomipramine and fluoxetine in isolated rat vas deferens: a relative potency measurement study. J Urol [Internet]. 2002;168:2716–9. Available from: http://www.ncbi.nlm.nih.gov/pubmed/12442016

70. Seifert R. How do basic secretagogues activate mast cells? Naunyn Schmiedebergs Arch Pharmacol. 2015;388:279–81.

71. Amin K. The role of mast cells in allergic inflammation. Respir Med [Internet]. 2012;106:9–14. Available from: http://dx.doi.org/10.1016/j.rmed.2011.09.007

72. Gupta K, Harvima IT. Mast cell-neural interactions contribute to pain and itch. Immunol Rev. 2018;282:168–87.

73. Kremer AE, Feramisco J, Reeh PW, Beuers U, Oude Elferink RPJ. Receptors, cells and circuits involved in pruritus of systemic disorders. Biochim Biophys Acta - Mol Basis Dis [Internet]. 2014;1842:869–92. Available from: http://dx.doi.org/10.1016/j.bbadis.2014.02.007

74. Azimi E, Reddy VB, Shade K-TC, Anthony RM, Talbot S, Pereira PJS, et al. Dual action of neurokinin-1 antagonists on Mas-related GPCRs. JCI Insight. 2016;1.

75. Steinhoff M, Buddenkotte J, Lerner EA. Role of mast cells and basophils in pruritus. Immunol Rev. 2018;282:248–64.

76. Ikoma A, Steinhoff M, Ständer S, Yosipovitch G, Schmelz M. The neurobiology of itch. Nat Rev Neurosci. 2006;7:535–47.

77. Yang S, Liu Y, Lin AA, Cavalli-Sforza LL, Zhao Z, Su B. Adaptive evolution of MRGX2, a human sensory neuron specific gene involved in nociception. Gene [Internet]. 2005;352:30–5. Available from: http://www.ncbi.nlm.nih.gov/pubmed/15862286

78. Folks DG, Warnock JK. Psychocutaneous disorders. Curr Psychiatry Rep. 2001;3:219–25.

79. Hautmann G, Lotti T. Psychoactive drugs and skin. J Eur Acad Dermatology Venereol. 2003;17:383–93.

80. Warnock JK, Morris DW. Adverse cutaneous reactions to antidepressants. Am J Clin Dermatol. 2002;3:329–39.

81. Ribeiro-Vaz I, Marques J, Demoly P, Polónia J, Gomes ER. Drug-induced anaphylaxis: A decade review of reporting to the Portuguese Pharmacovigilance Authority. Eur J Clin Pharmacol. 2013;69:673–81.

82. Weisshaar E, Szepietowski JC, Darsow U, Misery L, Wallengren J, Mettang T, et al. European guideline on chronic pruritus: In cooperation with the European dermatology forum (EDF) and the European academy of dermatology and venereology (EADV). Acta Derm Venereol. 2012;92:563–81.

83. Kaur R, Sinha VR. Antidepressants as antipruritic agents: A review. Eur Neuropsychopharmacol. 2018;28:341–52.

84. Ständer S, Böckenholt B, Schürmeyer-Horst F, Weishaupt C, Heuft G, Luger TA, et al. Treatment of chronic pruritus with the selective serotonin re-uptake inhibitors paroxetine and fluvoxamine: Results of an open-labelled, two-arm proof-of-concept study. Acta Derm Venereol. 2009;89:45–51.

85. Boozalis E, Khanna R, Zampella JG, Kwatra SG. Tricyclic antidepressants for the treatment of chronic pruritus. J Dermatolog Treat [Internet]. 2019;1–3. Available from: https://www.tandfonline.com/doi/full/10.1080/09546634.2019.1623369

86. Zylicz Z, Krajnik M, Sorge AA van, Costantini M. Paroxetine in the treatment of severe non-dermatological pruritus: A randomized, controlled trial. J Pain Symptom Manage. 2003;26:1105–12.

87. Goossens A, Linsen G. Contact allergy to antihistamines is not common. Contact Dermatitis [Internet]. 1998;39:38–9. Available from: http://doi.wiley.com/10.1111/j.1600-0536.1998.tb05817.x

88. Greenberg JH. Allergic contact dermatitis from topical doxepin. Contact Dermatitis [Internet]. 1995;33:281–281. Available from: http://doi.wiley.com/10.1111/j.1600-

0536.1995.tb00494.x

89. Greil W, Zhang X, Stassen H, Grohmann R, Bridler R, Hasler G, et al. Cutaneous adverse drug reactions to psychotropic drugs and their risk factors – a case-control study. Eur Neuropsychopharmacol [Internet]. 2019;29:111–21. Available from: https://doi.org/10.1016/j.euroneuro.2018.10.010

90. Calkin JM, Maibach HI. Delayed hypersensitivity drug reactions diagnosed by patch testing. Contact Dermatitis. 1993;29:223–33.

91. Simons FER. Advances in H 1 -Antihistamines . N Engl J Med. 2004;351:2203–17.

92. Rodríguez Del Río P, González-Gutiérrez ML, Sánchez-López J, Nuñez-Acevedo B, Bartolomé Álvarez JM, Martínez-Cócera C. Urticaria caused by antihistamines: Report of 5 cases. J Investig Allergol Clin Immunol. 2009;19:317–20.

93. Li HK, Rombach I, Zambellas R, Sarah Walker A, McNally MA, Atkins BL, et al. Oral versus intravenous antibiotics for bone and joint infection. N Engl J Med. 2019;380:425–36.

94. Murphy JL, Fenn N, Pyle L, Heizer H, Hughes S, Nomura Y, et al. Adverse Events in Pediatric Patients Receiving Long-term Oral and Intravenous Antibiotics. Hosp Pediatr. 2016;6:330–8.

95. Berroa F, Lafuente A, Javaloyes G, Cabrera-Freitag P, De La Borbolla JM, Moncada R, et al. The incidence of perioperative hypersensitivity reactions: A single-center, prospective, cohort study. Anesth Analg. 2015;121:117–23.

96. Gonzalez-Estrada A, Pien LC, Zell K, Wang XF, Lang DM. Antibiotics are an important identifiable cause of perioperative anaphylaxis in the United States. J Allergy Clin Immunol Pract [Internet]. 2015;3:101–105.e1. Available from: http://dx.doi.org/10.1016/j.jaip.2014.11.005

97. Sachs B, Dubrall D, Fischer-Barth W, Schmid M, Stingl J. Drug-induced anaphylactic reactions in children: A retrospective analysis of 159 validated spontaneous reports. Pharmacoepidemiol Drug Saf. 2019;28:377–88.

98. Iversen L, Gibbons S, Treble R, Setola V, Huang XP, Roth BL. Neurochemical profiles

of some novel psychoactive substances. Eur J Pharmacol [Internet]. 2013;700:147–51. Available from: http://dx.doi.org/10.1016/j.ejphar.2012.12.006

99. Tatsumi M, Groshan K, Blakely RD, Richelson E. Pharmacological profile of antidepressants and related compounds at human monoamine transporters. Eur J Pharmacol. 1997;340:249–58.

100. Kornhuber J, Tripal P, Gulbins E, Muehlbacher M. Functional Inhibitors of Acid Sphingomyelinase (FIASMAs). In: Handbook of experimental pharmacology [Internet]. 2013. p. 169–86. Available from: http://www.ncbi.nlm.nih.gov/pubmed/23579453%5Cnhttp://link.springer.com/10.1007/978-3-7091-1368-4

101. McQuade RD, Richlan K, Duffy RA, Chipkin RE, Barnett A. In vivo binding properties of non-sedating antihistamines to CNS histamine receptors. Drug Dev Res. 1990;20:301–6.

102. Kroeze WK, Hufeisen SJ, Popadak BA, Renock SM, Steinberg S, Ernsberger P, et al. HL-Histamine receptor affinity predicts short-term weight gain for typical and atypical antipsychotic drugs. Neuropsychopharmacology. 2003;28:519–26.

103. Roth BL, Sheffler DJ, Kroeze WK. Mood Disorders and Schizophrenia. Nat Rev Drug Discov. 2004;3:353–9.

104. Owens MJ, Knight DL, Nemeroff CB. Second-generation SSRIs: Human monoamine transporter binding profile of escitalopram and R-fluoxetine. Biol Psychiatry. 2001;50:345–50.

105. Eiser N. The effect of a β2-adrenergic agonist and a histamine H1-receptor antagonist on the late asthmatic response to inhaled antigen. Respir Med. 1991;85:393–9.

106. Martínez-Mir MI, Estañ L, Morales-Olivas FJ, Rubio E. Effect of histamine and histamine analogues on human isolated myometrial strips. Br J Pharmacol. 1992;107:528–31.

107. Kobayashi H, Hasegawa Y, Ono H. Cyclobenzaprine, a centrally acting muscle relaxant, acts on descending serotonergic systems. Eur J Pharmacol. 1996;311:29–

35.

108. Mestres J, Seifert SA, Oprea TI. Linking pharmacology to clinical reports cyclobenzaprine and its possible association with serotonin syndrome. Clin Pharmacol Ther [Internet]. 2011;90:662–5. Available from: http://dx.doi.org/10.1038/clpt.2011.177/nature06264

Table I – Classification of novel MRGPRX2 agonists by medical use, reuptake inhibition, antagonistic effects and inhibition of acid sphingomyelinase (FIASMA)

Agonist	Usage as	3D model	Reuptake inhibition	Antisero-tonergic	Antihista-minergic	Antidopa-minergic	Anticholi-nergic	Antiad-renergic	FIASMA	Ref.
Aminobenztropine		ARR								
Amitriptyline	Antidepressant	ARRM	SERT (+), NET (+)	+	++	o	o	o	+	56,64,98–100
Benztropine	Antispasmodic	ARR	DAT (+)	++	++	o	++	+	+	56,100
Chlorpheniramine	Antiallergic agent	ARRH	SERT (+), NET (o), DAT		++					56,99,101
Chlorpromazine	Antipsychotic	ARRHM	SERT (o), NET (o)	+	+	+	+	+	+	56,100,102,103
Chlorprothixene	Antipsychotic	ARRHM	SERT (o), NET (+), DAT	++	++	++	+	+	+	56,100
Citalopram	Antidepressant	ARRHM	SERT (++)		o		o	o		56,64,99,104
Clemastine	Antiallergic agent	ARRHM			++			o	+	56,100,105
Clemizole	Antiallergic agent	ARRH			+					56,106
Clomipramine	Antidepressant	ARRHM	SERT (++), NET (+)	+	+	o	+	+	+	56,64,99,100
Clozapine	Antipsychotic	ARRHM	SERT (o), NET (o)	++	++	+	++	++		56,102,103
Cyclobenzaprine	Antispasmodic	ARRM	SERT (+), NET (+)	++				+	+	56,100,107,108
Cyproheptadine	Antiallergic agent	ARRM	NET (o)	++	++	+	++		+	56,100
Desipramine	Antidepressant	ARRM	SERT (++), NET (++)	o	+		+	+	+	56,99,100
Diltiazem	Antispasmodic*	ARRM								
Fluoxetine	Antidepressant	ARRH	SERT (++), NET (o)	+	o		o		+	56,64,98–
Imipramine	Antidepressant	ARRM	SERT (+), NET (+)	+	+		+	o	+	56,64,99,100
Paroxetine	Antidepressant	ARRH	SERT (++), NET (o), DAT				+		+	56,64,99,100,104

*Diltiazem is used in angina and hypertensive disorders (vasodilatation); A = Amino group, R = benzene ring, M = hydrophobic center, H = halogen substituent, SSRI = selective serotonin reuptake inhibitor, TCA = tricyclic antidepressant, SERT = serotonin transporter, NET = norepinephrine transporter, DAT = dopamine transporter; o (K_i = 0.2–20 nM), + (K_i = 21–200 nM), ++ (K_i = 201–2000 nM).

FIGURES LEGENDS

Fig.1: Pharmaceutically active compounds activate MRGPRX2.

(A) Maximum ratio of intracellular Ca^{2+}-dependent fluorescence intensity (FI) upon stimulation of MRGPRX2-expressing HEK293 cells by 18 pharmaceutically active compounds at 30 µM and C48/80 as positive control (10 g/mL). Maximum FI is equivalent to the peak point of transient Ca^{2+}-dependent fluorescence of Fura-2-AM ratio at 340 nm and 380 nm shown in Fig.S2. Bars represent mean+SEM (n = 3-6). (B) Transient Ca^{2+}-dependent fluorescence intensity (FI, 340/380 nm) in MRGPR-expressing HEK293 cells and empty vector control (MOCK) upon stimulation with clomipramine, paroxetine, desipramine (30 µM) and C48/80 (10 µg/mL). Arrows indicate addition of stimulus. Graphs represent mean±SEM (n = 3-6). (C) Average concentration-response curves of clomipramine, paroxetine, desipramine and C48/80 showing the measured maximum FI for the respective concentration (mean±SEM) plotted with a non-linear regression fit to determine the half-maximal effective concentration (EC_{50}) in MRGPRX2-expressing HEK293 cells (n = 3-4). MOCK cells were used as control (n = 3-4); highest p-values are depicted: **** $p<0.0001$, * $p<0.05$ (Two-way ANOVA with post-hoc Sidak's multiple comparisons test). (D) Concentration-response curves of clomipramine, paroxetine, and desipramine in β-arrestin assays (n = 3, mean±SEM) at the MRGPRX2 receptor using CHO cells recombinantly expressing the receptor.

Fig.2: Novel MRGPRX2 agonists, sharing structural commonalities, are cationic amphiphilic drugs.

3D pharmacophore modeling of agonists with Maestro Software (Schroedinger, used to highlight the molecular surface and the electrostatic potential thereof) revealed structural similarities: all 18 agonists feature an aliphatic protonatable amino group and a lipophilic group of two benzene rings (ARR); 12 out of 18 substances additionally have a hydrophobic center (ARRM) and 10 out of 18 substances exhibit a halogen substituent on one of the

aromatic rings (ARRH). Structural features: Amino group (A), two benzene rings (RR), hydrophobic center (M), halogen substituent (H).

Fig.3: MRGPRX2-dependent activation and degranulation of human mast cells by the cationic amphiphilic drugs clomipramine, paroxetine, and desipramine.

(A) Average concentration-response curves of clomipramine, paroxetine, and desipramine on LAD2 cells showing measured maximum fluorescence intensity (FI, 340/380 nm) for the respective concentration (n = 3-5, mean±SEM) plotted with a non-linear regression fit to determine the half-maximal effective concentration (EC_{50}). (B) Concentration-dependent degranulation of LAD2 cells (n = 3-5) measured by β-hexosaminidase release upon stimulation by clomipramine, paroxetine, and desipramine (concentration as indicated). Degranulation is defined as the brutto release of β-hexosaminidases in % of total content, SP (30 µM) was used as positive control. One-way ANOVA with post-hoc Tukey's multiple comparisons test was used for statistical analysis. (C) Elimination of MRGPRX2 in LAD2 cells by CRISPR-Cas9 (LAD2 MRGPRX2 KO) decreased degranulation upon stimulation with clomipramine, paroxetine and desipramine (50 µM) in comparison to wild-type LAD2 cells (LAD2 WT). C48/80 (10 µg/mL) and Tween20 (2%) were used as positive control. Two-way ANOVA with Sidak's multiple comparisons test was used for statistical analysis (n = 4). (D) Concentration-dependent degranulation of primary human skin mast cells (hsMCs, *n* = 3 donors) measured by β-hexosaminidase release upon stimulation by clomipramine, paroxetine, and desipramine (concentration as indicated) or SP (10 µM) as positive control. A Kruskal-Wallis test with post-hoc Dunn's multiple comparisons test was applied. For all subfigures: bars represent mean+SEM; **** p<0.0001, *** p<0.001, ** p<0.01, * p<0.05.

Fig.4: Clomipramine, paroxetine, and desipramine mediate murine mast cell activation and degranulation – potentially via MRGPRB2.

(A) Average time course of Ca^{2+}-dependent fluorescence intensity (FI, 358/391 nm) on primary peritoneal murine mast cells (mpMCs, *n* = 3 donors) treated with clomipramine

(75 µM), paroxetine (100 µM), or desipramine (150 µM) followed by SP (50 µM) and C48/80 (15 µg/mL). Bars indicate application period; graphs represent mean±95% confidence interval of N cells. (B) Scatterplots of the ratio increases for mpMCs responding to clomipramine, paroxetine, or desipramine and SP or C48/80, respectively. Within the scatterplots, every dot reflects a single cell. Non-parametric Spearman correlation (r) and two-tailed p values were computed: $p<0.001$ for all scatterplots. (C) Concentration-dependent degranulation of mpMCs measured by β-hexosaminidase release upon stimulation by clomipramine, paroxetine, and desipramine (concentration as indicated). Bars represent mean+SEM (*n* = 3 donors); *** $p<0.001$, ** $p<0.01$, * $p<0.05$ (Kruskal-Wallis test with post-hoc Dunn's multiple comparisons test). SP (10 µM) was used as positive control. (D) Evans Blue stained extravasation 15 min after intradermal ear injection of clomipramine (100 µg) or C48/80 (100 µg) and PBS as negative control in C57BL/6N mice. Quantified by measurement of absorbance at 600 nm after Evans blue extraction with formamide. Bars represent mean±SEM, each dot reflects one single mouse (*n* = 7-8 mice); ** $p<0.01$, * $p<0.05$ (paired t-test). (E+F) Time course of Ca^{2+}-dependent fluorescence intensity (FI, 358/391 nm) on HEK293T cells transiently transfected with (E) *Mrgprb2* and (F) empty vector control (MOCK) upon stimulation by clomipramine, paroxetine, and desipramine at a concentration of 50 µM as well as C48/80 (10 µg/mL), NPFF (10 µM) and ionomycin (2 µM) as controls. Bars indicate application period; graphs represent mean (colored line) ± 95% confidence interval (in grey) of N cells (n = 4 for (E) and n = 3-4 for (F)).

Fig.5: Clomipramine, paroxetine, and desipramine induce scratching behavior in mice. (A) Scratch bouts within 30 min after intradermal injection (50 µL) of clomipramine, paroxetine, and desipramine with PBS as negative and C48/80 as positive control, each 100 µg per mouse in C57BL/6N mice (*n* = 7 mice, Brown-Forsythe and Welch ANOVA with post-hoc Dunnett's T3 multiple comparisons test). (B) Dose-dependent scratching behavior after intradermal injection of 50 µL of the indicated concentrations of clomipramine in the neck of C57BL/6N mice (Latin square counterbalancing, *n* = 16 mice, Kruskal-Wallis test with

post-hoc Dunn's multiple comparisons test). (C-E) Scratch bouts within 30 min after intradermal injection of 100 µg clomipramine (C, *n* = 9-10 mice, unpaired t test with post-hoc Welch's correction), paroxetine (D, *n* = 11-12 mice, unpaired t test), or desipramine (E, *n* = 10 mice, unpaired t test with post-hoc Welch's correction) in C57BL/6N and MRGPRB2-mutant mice. For all subfigures: Bars represent mean±SEM, each dot reflects a single mouse, **** p<0.0001, *** p<0.001, ** p<0.01, * p<0.05.

Fig.6: Intradermally applied clomipramine evokes an activation of human skin mast cells.

(A) Wheal-and-flare reaction 20 min after intradermal injection of 50 µL of clomipramine (5 mM) in comparison to vehicle control in five healthy volunteers (*n* = 5, Two-way ANOVA with post-hoc Sidak's multiple comparison test). (B) Laser speckle contrast imaging of the skin of the volar forearm 3 min and 20 min after intradermal injection of clomipramine (Clomi., *n* = 5, paired t test). (C) Example of flare development measured by laser speckle contrast imaging 3 min after provocation with 5 mM clomipramine in comparison to vehicle control. (D) Maximal itch intensity within 30 min upon provocation with clomipramine (*n* = 5, paired t test), ascertained by means of a visual analogue scale (VAS, 0-100 mm). (E) Time course of itch sensation in *n* = 5 subjects. Itch intensity was self-reported by subjects on a VAS every single minute. For subfigures A-D: Bars represent mean±SEM, each dot reflects a single subject, **** p<0.0001, * p<0.05.

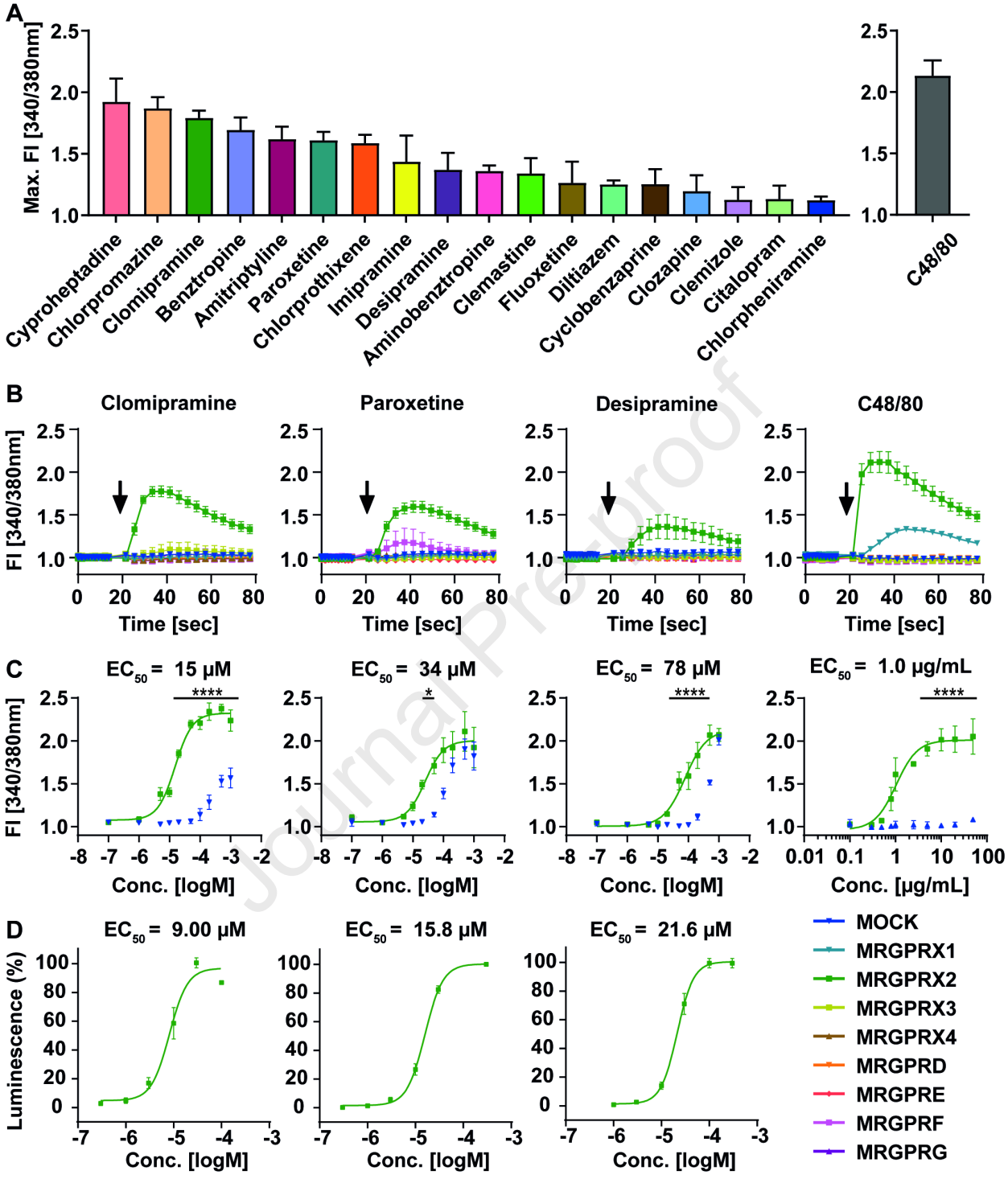

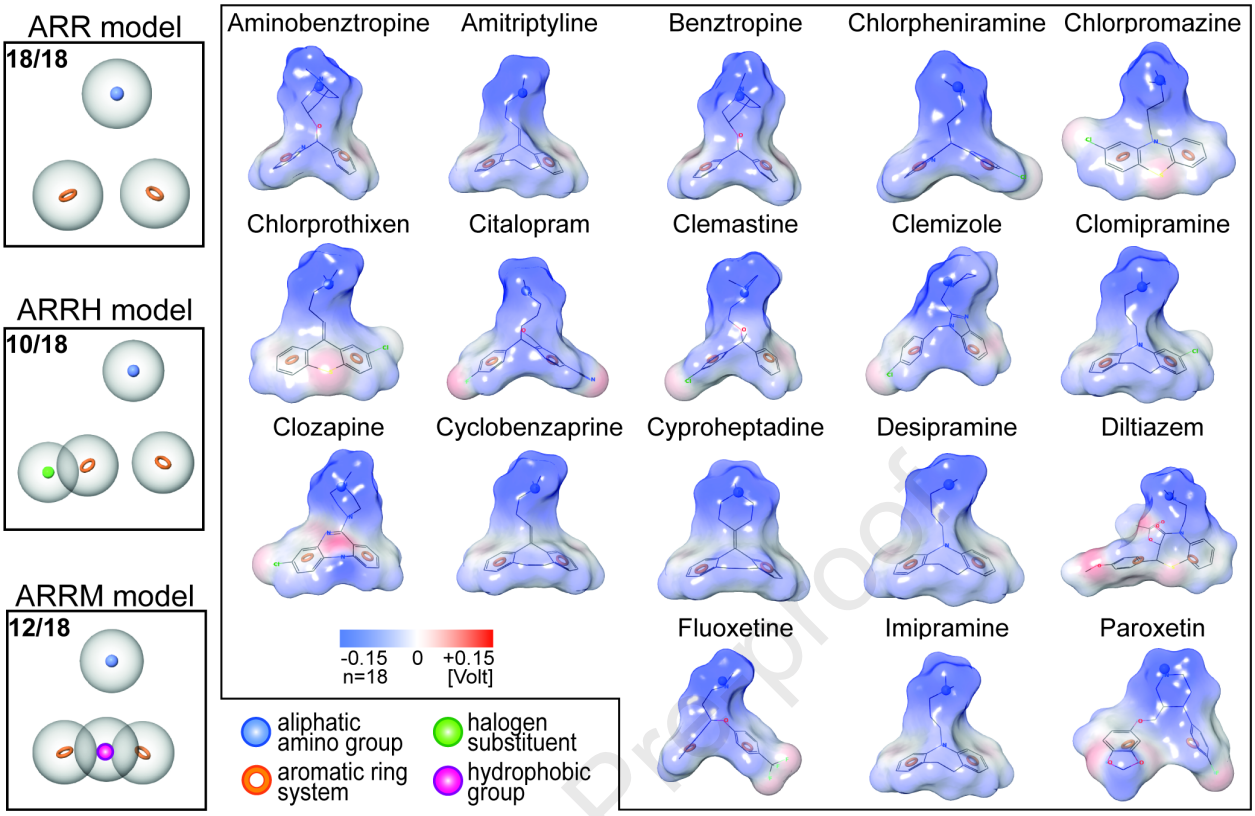

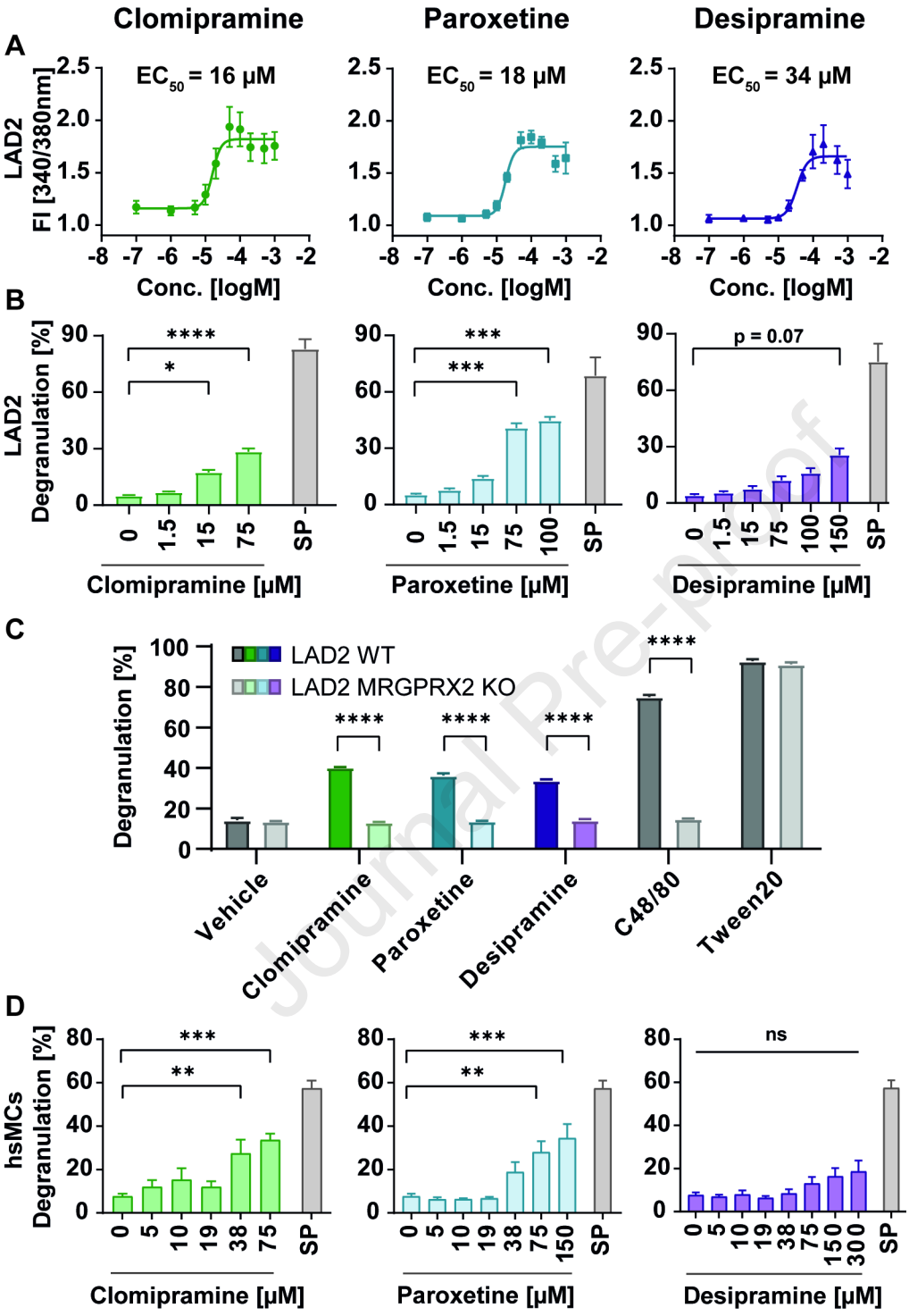

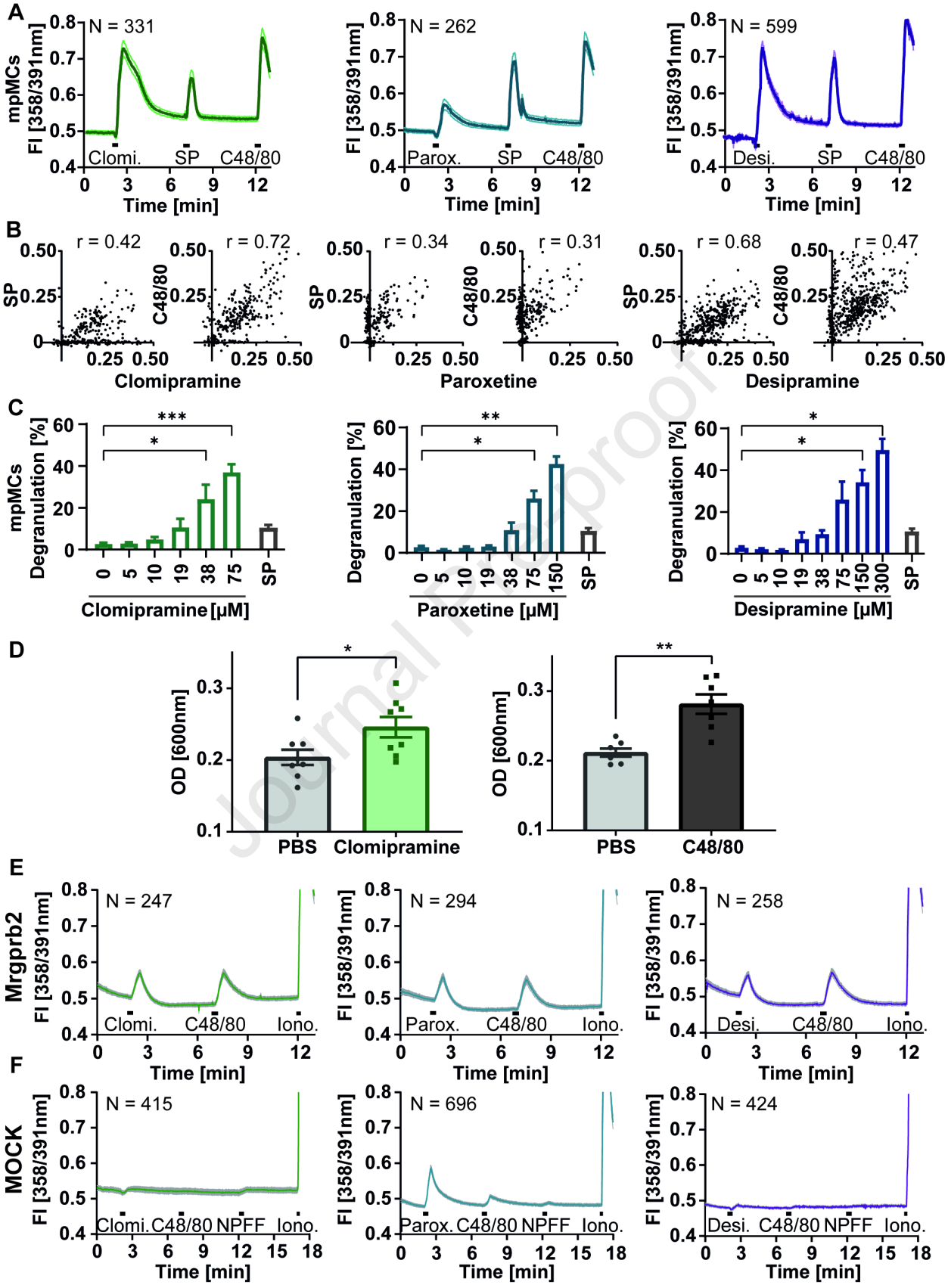

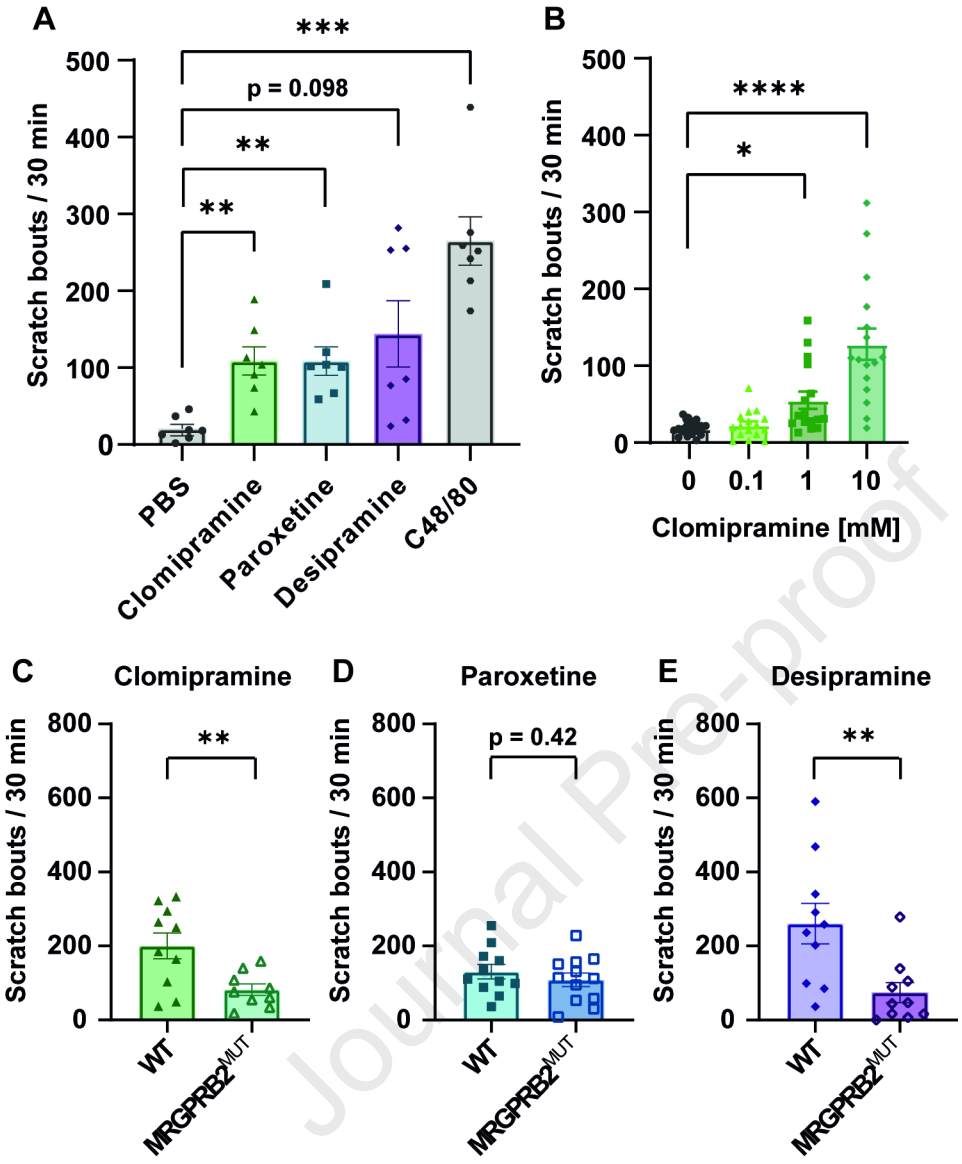

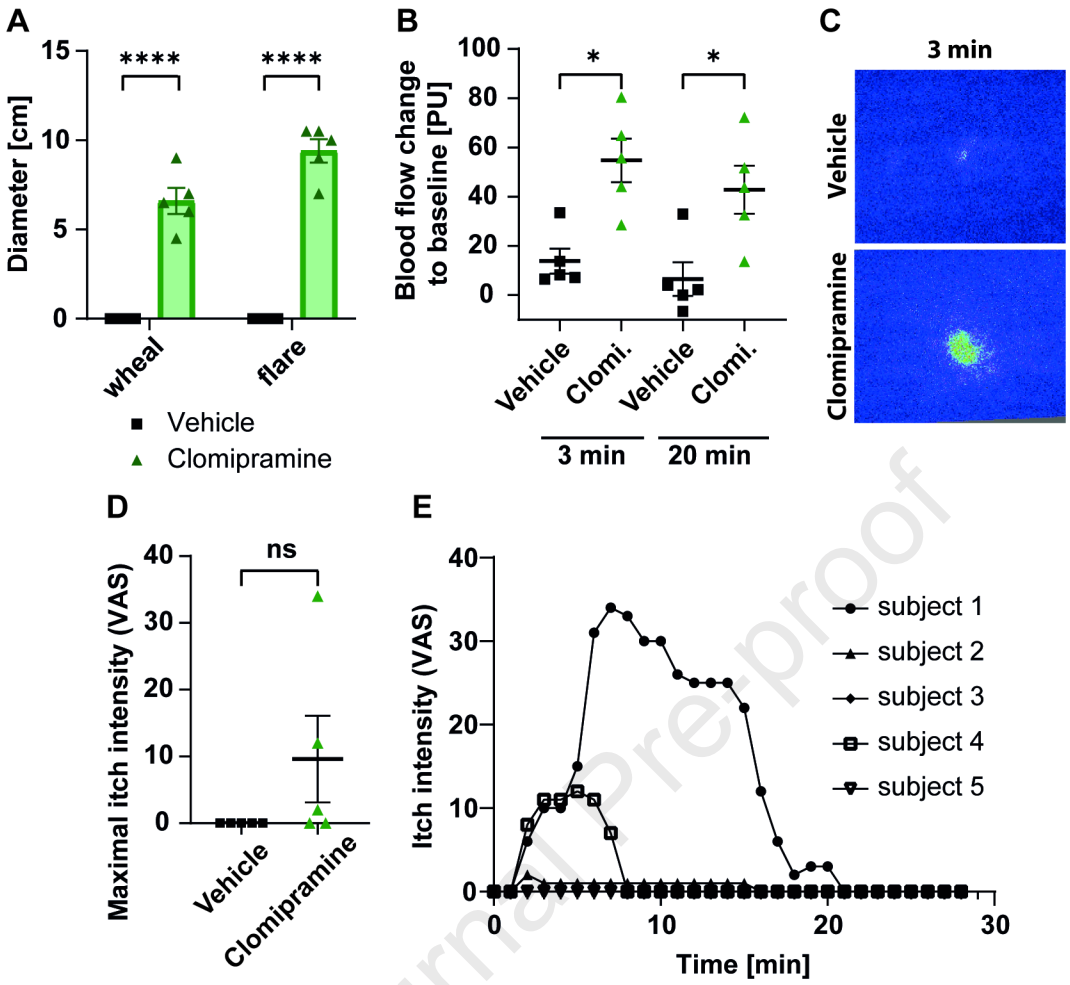

SUPPLEMENT/ONLINE REPOSITORY

Materials and methods

Isolation and culture of human skin mast cells

In brief, human breast skin or eyelids from plastic reduction surgeries were digested in 2.4 U/mL dispase type II (Roche) over night at 4 °C. The epidermis was removed, the skin was minced with scissors and further digested for 1 h in Dulbecco's phosphate-buffered saline (DPBS) containing Ca^{2+} and Mg^{2+} (Life Technologies) supplemented with 1% Pen/Strep, 5% FBS, 2.5 µg/mL amphothericin (Biochrom, Berlin, Germany), 5 mM $MgSO_4$, 10 µg/mL DNase I (Roche), 0.75 mg/mL hyaluronidase (H-3506, Sigma-Aldrich) and 1.5 mg/mL collagenase (type II, Worthington Biochemical Corp., Lakewood, NJ, USA) at 37 °C with shaking. The cell suspension was filtered via 300 µm and 40 µm sieves (Retsch, Haan, Germany) followed by centrifugation at 300 g for 15 min at 4 °C and the digestion cycle was repeated once. Cells were washed in DPBS without Ca^{2+} and Mg^{2+} (Life Technologies). MCs were isolated by CD117 positive MACS enrichment (Miltenyi, Bergisch Gladbach, Germany) and cultured in basal Iscove's medium supplemented with 1% Pen/Strep, 10% FBS, 1% non-essential amino acids (all Life Technologies) and 226 µM α-monothioglycerol. Cells received recombinant human IL-4 (20 ng/mL) and hSCF (100 ng/mL) (both Peprotech) after 24 h in culture. Cells were cultured 1-2 weeks prior to the degranulation assay at 1.0×10^6 cells/mL with addition of IL-4 and SCF twice a week.

Cloning of human MRGPRs and murine Mrgprs

Cloning primers for human *MRGPRs* (supplementary table 1) were designed to introduce a 5'EcoRI and a 3'Xhol cleavage site. The cloning primers for *Mrgpra1* (supplementary table 1), were designed to create a 5´SmaI and 3´BglII restriction site. For *Mrgpra3* and *-b2* the primers introduced a 5´SmaI and a 3´BamHI restriction site. Amplification products were loaded onto a 2% agarose gel supplemented with Midori Green Advanced (Nippon Genetics Europe, Dueren, Germany) and separated for 30 min at 90 V. Visualization was conducted on a Gel Doc™XR+ Gel Documentation System (Bio-Rad Laboratories, Hercules, CA, USA).

Products of the expected size were extracted and purified using the NucleoSpin® Gel and PCR Clean-up kit (Macherey-Nagel, Düren, Germany). Human *MRGPRs* were cloned into the pMP71 plasmid containing an IRES followed by green fluorescent protein (GFP), allowing detection of transduced cells.[46,47] Murine *Mrgprs* were cloned into the mYFP-fusion plasmid producing MRGPR-YFP fusion proteins. pMP71 plasmid and amplified *MRGPRs* were cut with EcoRI-HF and XhoI (New England Biolabs, Ipswich, MA, USA). mYFP-fusion plasmid and amplified murine *Mrgpra1* were cut with BglII and SmaI whereas the amplified *Mrgpra3* and *b2* were cut with BamHI and SmaI. After visualization by agarose gel electrophoresis and purification, ligation was performed using the T4 DNA ligase (Thermo Fisher Scientific) at 16°C overnight and transformed NEB 5-alpha chemically competent *E.coli* (New England Biolabs). Transformed bacteria were plated on agar plates supplemented with ampicillin (100 mg/mL) for pMP71 plasmid or kanamycin (50 mg/mL) for mYFP-fusion plasmid. After incubation for 12 h at 37 °C clones were picked and grown in LB media supplemented with ampicillin or kanamycin overnight. Plasmids were isolated using the Qiagen Plasmid Purification Kit (Qiagen, Hilden, Germany).

Multi-cell fluorometric measurement of cytosolic calcium levels

HEK293 cells were harvested, washed three times with wash buffer composed of Hank's balanced salt solution (HBSS) containing 0.2% bovine serum albumin (BSA) and 10 mM HEPES, and counted. Cells were incubated with 1 µg/µL Fura-2 AM (Life Technologies and Biotium, dissolved in DMSO) in HBSS containing BSA, HEPES and 0.25% pluronic acid F-127 (Life Technologies), for 60 min at 37 °C and washed three times with wash buffer. Thereafter, cells were resuspended in wash buffer to a final concentration of 5×10^5 cells per 100 µL. Five minutes prior to calcium measurements, cells were transferred to a 96-cell UV-STAR® micro plate (Greiner Bio-One, Kremsmünster, Austria) with 5×10^5 cells per well and pre-warmed to 37 °C. Analyses were performed in a microplate fluorimeter with integrated pipetting system (BMG Labtech NOVOstar, Offenburg, Germany) at 340 and 380 nm for excitation and 510 nm for emission. For every experiment, apertures of both wavelengths

were adjusted to yield the same signal intensity, resulting in a baseline ratio of 1. Emission was recorded every 1.5 s with 10 flashes per interval. After baseline measurement for 21.4 s, the integrated pipetting system automatically added substances to the cell suspension with a velocity of 360 µL/s. Shifts in emission intensity were recorded every 4 s for 60 s. Analysis and calculation of the 340 nm/380 nm ratio (FI 340/380 nm) was conducted in Excel 2016 (Microsoft Cooperation, Redmond, WA, USA).

Calcium microfluorimetry of single cells

Fura-2AM dye was mixed with pluronic® F-127 (final concentration 0.02%, Biotrend, Cologne, Germany) and diluted to 3 µM in external solution. Cells were loaded with this dye for about 30 min at 37 °C and 5% CO_2 and washed in pure external solution for 10 min at room temperature. On an inverted microscope, the samples were excited at 358 and 391 nm with a Polychrome V monochromator (Till Photonics, Graefelfing, Germany) at 1 Hz. A gravity driven and software-controlled common outlet perfusion system generated a continuous superfusion of the cells throughout the experiment at a rate of 0.5 mL/min.[49] A peltier-cooled slow-scan CCD camera collected the fluorescence emission above 440 nm. The TillVision software was used to control the experiments, to analyze the data and to calculate the fluorescence ratio (FI 358/391 nm) for all regions of interest after background subtraction. The area under the curve (AUC) of the ratio within one minute after start of application was analyzed in comparison to control periods. Protocols contained a final application of KCl (60 mM) for primary cells and of ionomycin (2 µM) for transfected HEK293T to acquire a maximum response and to discard nonresponsive cells; positive calcium responses were defined as ratio increases above 0.1. An application period of 30 s was applied for clomipramine, paroxetine, desipramine, NPFF, chloroquine, ATP, C48/80, substance P and carvacrol as well as 20 s for KCl and ionomycin and 10 s for capsaicin (all: Sigma-Aldrich, except NPFF: Genscript Biotech, Piscataway Township, NJ, USA). All calcium microfluorimetry experiments were performed in extracellular solution, consisting of

145 mM NaCl, 5 mM KCl, 1.3 mM $CaCl_2$, 1 mM $MgCl_2$, 10 mM HEPES, 10 mM glucose (adjusted to the physiological pH 7.4; all: Carl Roth, Karlsruhe, Germany).

β-hexosaminidase release assay

LAD2 cells were fed the day before stimulation. Next day, 1 x 10^5 cells were incubated with final concentrations of clomipramine, paroxetine and desipramine ranging from 1.5 to 100 µM in a PIPES CM buffer (25 mM Pipes, 119 mM NaCl, 5 mM KCl, 2.8 mM CaCl2, 1.4 mM MgCl2; pH 7.4) supplemented with 0.1% BSA at 37 °C for 30 min. Incubation with substance P (30 µM, Sigma-Aldrich) was used as positive control. Unstimulated cells served as control for spontaneous release and lysed cells (Triton-X 100, 1%, Sigma-Aldrich) as control for total content. Supernatants were collected and rapidly frozen at -80 °C. Thawed lysates (20 µL) were equally mixed with 4-nitrophenyl N-acetyl-β-D-glucosaminide (Sigma-Aldrich: pNAG, in 0.05 M citrate buffer, pH 4.5) and incubated at 37 °C for 1 h. Reaction was stopped by adding 200 µL of sodium carbonate buffer (0.05 M, pH 10.0) and absorbance was measured in a plate reader. The percentage of specific release was calculated as follows: (100 / content total) * release stimulated = release in % of total content (set equal to 100%).

For β-hexosaminidase release assay in MRGPRX2-deficient LAD2 cells, knockout cells and control cells (LAD2 wild-type (WT)) were seeded (0.25 x 10^5 cells per well) and treated with different concentrations of clomipramine, paroxetine, desipramine ranging from 12.5 µM to 100 µM for 30 min at 37° C and 5% CO_2. C48/80 (10 µg/mL) and Tween-20 (2%) were used as positive controls for MRGPRX2-dependent and MRGPRX2-independent degranulation, respectively. After incubation, cells were pelleted, supernatants were harvested, and cells were lysed using 0.1% Triton-X100. The β-hexosaminidase in both supernatants and in cell lysates were quantified by hydrolysis of pNAG in 0.1 M sodium citrate buffer (pH 4.5) for 90 min at 37° C. The percentage of β-hexosaminidase release was calculated as a percent of total content.

HsMCs and mpMCs were fed the day before stimulation with medium. Next day, 5 × 10^5 cells were seeded into a 96-well plate in a total volume of 50 µL of warm HEPES-Tyrodes buffer.

The cells were incubated with final concentrations of clomipramine, paroxetine and desipramine ranging from 5 to 300 µM, substance P (10 µM, Sigma-Aldrich), IgE (1 µg/mL, Merck KGaA), Tyrodes buffer or ionomycin (1 µM, Sigma-Aldrich) for 1 h at 37 °C. The cells stimulated with IgE were then separately treated with anti-IgE (1 µg/mL, Bethyl Laboratories, Montgomery, TX, USA) for 1 h at 37 °C. After stimulation, the cells were centrifuged and 50 µL of supernatant was collected. The cells were lysed in 100 µL of distilled water and lysates were rapidly frozen at the -80 °C. After thawing, 50 µL of lysates and supernatants were incubated for 1 h at 37 °C with the same amount of 4-methylumbelliferyl N-acetyl-β-D-glucosaminide (Sigma-Aldrich) diluted in citrate buffer (pH 4.5) to measure the level of secreted and intracellular hexosaminidase. Reaction was stopped by adding 100 µL of sodium carbonate buffer (pH 10.7), and fluorescence was measured at 460 nm and excitation at 355 nm for 0.1 s. The percentage of β-hexosaminidase release was calculated as (optical density [OD] of lysates + OD of supernatants)/OD of supernatants x 100.

Behavioral scratch assay

For the automated detection of scratch movements in mice, small polytetrafluoroethylene-coated magnets (size: 5x2mm, VWR, Radnor, PA, USA) were subcutaneously implanted into the hind paws of C57BL/6N mice one week before behavioral tests. For scratch experiments, animals were accustomed to the measurement cages at least 60 min before intradermal injection of 50 µL DPBS or the respective pruritogen into the nape using a 30G fine dosage syringe (B. Braun, Melsungen, Germany). Behavioral experiments were conducted on five consecutive days with injection of PBS on the first day, followed by application of clomipramine (100 µg, 5.69 mM), paroxetine (100 µg, 5.34 mM), desipramine (100 µg, 6.60 mM) and C48/80 (100 µg, 2 g/L). Evaluation of dose-dependent scratching behavior in response to intradermal application of 0 mM (PBS only), 0.1 mM, 1 mM and 10 mM clomipramine was done using the diagram-balanced Latin Square method. Mice were injected on consecutive days in the neck. Repetitive injections did not cause a visible damage of the skin, which was verified each day before intradermal injection. Immediately

after injection, scratching was assessed for 30 min. Scratches were automatically detected as the movement of the implanted magnets induced electric currents through two coils placed around the cage. Electric signals were recorded using oscillography. Recordings were controlled and stored using SiMon (V2.0, Academic Medical Center, University of Amsterdam) and analyzed thereafter using Scratch Analysis (V1.13, Academic Medical Center, University of Amsterdam). Movements with a frequency between 10–20 Hz, an amplitude above 300 mV and a minimum of 4 repetitions were classified as scratching. This magnet-based recording technology has a positive predictive value of 95 % at a sensitivity of 50% and a negative predictive value of 72% as shown before.[50]

For MRGPRB2-mutant and control mice, the day prior to the experiment, mice were acclimated in behavioral test chambers once for thirty minutes before being subjected to a series of three mock injections with 5-min break periods in between. On the day of the experiment, animals were habituated to the behavioral chamber for 10 minutes before injection. Clomipramine, paroxetine, or desipramine (each 100 μg in a 50 μl volume) were then injected to the nape of necks subcutaneously and mouse behavior was assessed for a total of 30 minutes. A total number of scratching bouts (defined as a lifting of either hind paw to scratch at the nape and replacing the paw onto the floor or to the mouth) was quantified within the 30-min observation period. All behavioral tests were performed and scored by experimenter who were blinded to the animal genotypes.

Tables

Supplementary table I – Primers used for cloning of *hsMRGPRs* and *mmMrgprs*

Gene	Primer direction	Primer Sequence (5' → 3') *
EcoRI-*hsMRGPRX1*-XhoI	FW	CCGGAATTCAGC**ATG**GATCCAACCATCTCAACC
	RV	CCGCTCGAGTCC**TCA**CTGCTCCAATCTGCTTCC
EcoRI-*hsMRGPRX2*-XhoI	FW	CCGGAATTCAGC**ATG**GATCCAACCACCCCGGCCT
	RV	CCGCTCGAGTCT**CTA**CACCAGACTGCTTCTCGA
EcoRI-*hsMRGPRX3*-XhoI	FW	CCGGAATTCAGC**ATG**GATTCAACCATCCCAGT
	RV	CCGCTCGAGTCC**TCA**CTGCTCCAATCTGCTTC
EcoRI-*hsMRGPRX4*-	FW	CCGGAATTCAGC**ATG**GATCCAACCGTCCCAGT

XhoI	RV	CCGCTCGAGCCC**TCA**TGGCCCCAATCTGCTT
EcoRI-*hsMRGPRD*-XhoI	FW	CCGGAATTCAGC**ATG**AACCAGACTTTGAATAG
	RV	CCGCTCGAGTCT**TCA**AGCCCCCATCTCATTGGT
EcoRI-*hsMRGPRE*-XhoI	FW	CCGGAATTCCCC**ATG**ATGGAGCCCAGAGAAGC
	RV	CCGCTCGAGGGC**TCA**GGCTGCTATGTCCAC
EcoRI-*hsMRGPRF*-XhoI	FW	CCGGAATTCGAG**ATG**GCTGGAAACTGCTCCTGG
	RV	CCGCTCGAGGTC**TCA**GGAGGCGTTCCCCG
EcoRI-*hsMRGPRG*-XhoI	FW	CCGGAATTCAGG**ATG**TTTGGGCTGTTCGGCCTC
	RV	CCGCTCGAGCAC**TTA**TAGGAGACCCATGGGCAGGG
Sma1-*mmMrgpra1*-BglII	FW	GGGGGGGAAAGCAGCACCTGTGCAGGGTTTCTAG
	RV	CGCAGATCTTGGCTCTGATTTGCTTCTTGACATCTCCAC
Sma1-*mmMrgpra3*-BamHI	FW	GGGGGAGAAAGCAACACCAGTGCAGGGTTTCTG
	RV	CGGATCCCGGCTCTGCTTTGTTTCTTGACATCTCCAC
Sma1-*mmMrgprb2*-BamHI	FW	GGGAGTGGAGATTTCCTAATCAAGAATCTAAGCACCTC
	RV	CGGATCCGCTGCAGCTCTGAACAGTTTCCAGTTCTTC

* Start- and Stop codons are displayed in bold and restriction sites are underlined. For murine constructs, Start and Stop codons are located in the plasmid's backbone.

Supplementary table II – Primers used for quantitative real-time PCR

Gene	**Primer direction**	**Primer Sequence (5' → 3')**	**Product Size**
hsMRGPRX1	FW	CGGCCGCCTTATATATTCCCT	287 bp
	RV	ACCAAGCAGAATCAGCACCA	
hsMRGPRX2	FW	GCCCATCTGGTATCGC	429 bp
	RV	GGGTTGGCACTGCTGTTAAGA	
hsMRGPRX3	FW	CCGACTTCCTCTTCCTTAGCG	229 bp
	RV	CAGAGCAGGACACACATGACT	
hsMRGPRX4	FW	TCTGGTTTGCATGTCCCTGT	94 bp
	RV	CTGCCTATTTTGACGCTGCC	
hsMRGPRD	FW	CCGTGGAGTCAGCCCTAAAC	157 bp
	RV	CAGAAGGGGTTCCTGTGCAT	
hsMRGPRE	FW	CGGAACCTGCTCTGGTACAT	99 bp
	RV	CAGGCAGAAGTAGACGACGG	
hsMRGPRF	FW	GGCAACAGGAACAAGATGT	250 bp
	RV	GAAGAGGTAGCCCACATCGG	
hsMRGPRG	FW	GCGTGGTCCTCTTTGTCTGG	128 bp
	RV	CAGGCTCCAGTAGAAGACCG	
hsHPRT	FW	AGCCAGACTTTGTTGGATTTGA	131 bp
	RV	GGCTTTGTATTTTGCTTTTCCAGT	
mmMrgpra1	FW	GAATGGGGGAAAGCAGCACC	297 bp
	RV	GCAGTATGGAATCTATGATGTGACC	

mmMrgprb2	FW	CCCTGGTTGGGATGGGACTA	267 bp
	RV	ACAAGCAGCGCTCAATGCTA	
mmMrgpra3	FW	ATCCTTCCTTCTACACAAGCCA	70 bp
	RV	CTGCACTGGTGTTGCTTTCTC	
mmHPRT	FW	ACAGGCCAGACTTTGTTGGAT	150 bp
	RV	ACTTGCGCTCATCTTAGGCT	

Figure legends

Fig.S1: MRGPR-overexpressing HEK293 model.

(A) Stable (over)expression of the eight human MRGPRs, MRGPRX1-4 and D-G, in HEK293 cells verified by detection of the respective mRNA in qPCR (n = 3). MRGPR-expressing cells were compared to an empty vector control (MOCK) and HEK293 cells (untreated). (B) Ca^{2+} mobilization assays with known agonists for MRGPRX1 (Bam8-22, 2 µM), MRGPRX2 (C48/80, 10 µg/mL), and MRGPRX4 (DC, 100 µM) as well as addition of PBS as negative control. Graphs represent mean±SEM (n = 3).

Fig.S2: Activation potential of newly discovered MRGPRX2 agonists.

(A) Transient Ca^{2+}-dependent fluorescence intensity (FI, 340/380 nm) in MRGPRX2-expressing HEK293 cells (n = 3-6) and empty vector control (MOCK, n = 2-3) upon stimulation with respective compounds (30 µM). Arrows indicate addition of stimulus; graphs represent mean±SEM depicted with a 2D structure of the compound and sorted according to the response. (B) Hierarchical cluster analysis of novel agonists by their maximum FI at 30 µM with average group linkage identifying four main groups with different MRGPRX2 activation potential denominated strong, intermediate, weak and very weak. (C) Average concentration-response curves of strong/intermediate and (very) weak agonists showing measured maximum FI for the respective concentration plotted with a non-linear regression fit to determine the half-maximal effective concentration (EC_{50}) (MRGPRX2: n = 3, MOCK: n = 2-3). (D) Correlation of the maximum FI upon stimulation of MRGPRX2-expressing HEK293 cells and the EC_{50} of the respective compound. Within the scatterplot, every dot

reflects a tested compound. Non-parametric Spearman correlation (r) and the two-tailed p-value were computed.

Fig.S3: MRGPRX2-dependent activation of human mast cells (continuation).

(A) Maximum ratio of intracellular Ca^{2+}-dependent fluorescence intensity (FI) upon stimulation of LAD2 cells by 12 pharmaceutically active compounds at a concentration of 30 µM and C48/80 as positive control (10 µg/mL). Bars represent mean+SEM (n = 3). (B) Correlation of maximum ratio of FI upon stimulation of LAD2 and MRGPRX2-expressing HEK293 cells. Within the scatterplot, every dot reflects a tested compound. Parametric Pearson correlation (r) and two-tailed p value were computed. (C) LAD2 cell viability depending on agonist concentration of clomipramine, paroxetine, and desipramine detected by flow cytometry. Viable cells were classified as $PI^-AnnexinV^-$ cells. Bars represent mean+SEM (n = 3-5).

Fig.S4: Clomipramine, paroxetine, and desipramine stimulate primary sensory neurons and activate MRGPRA1 but presumably not MRGPRA3.

(A) Average time course of Ca^{2+}-dependent fluorescence intensity (FI, 358/391 nm) in dissociated, 1-day cultured primary murine dorsal root ganglion (DRG) neurons. Cells were stimulated with clomipramine (Clomi., 100 µM), paroxetine (Parox., 25 µM), or desipramine (Desi., 100 µM) and TRPA1 agonist carvacrol (Carv., 100 µM), TRPV1 agonist capsaicin (Cap., 200 nM) as well as potassium chloride (KCl, 60 mM) as positive control. Bars indicate application period; graphs represent mean±95% confidence interval of N cells in one representative experiment out of three. (B) Venn diagrams illustrating the overlap of cells responding to either one or several of the stimuli applied. (C) Average cytosolic Ca^{2+} transients in HEK293T cells transfected with either *Mrgpra1*, *Mrgpra3* or empty vector control (MOCK). Cells were stimulated with clomipramine (Clomi., 50 µM), paroxetine (Parox., 50 µM), or desipramine (Desi., 50 µM) and NPFF (10 µM, MRGPRA1 agonist), C48/80 (10 µg/mL, MRGPRB2 agonist), chloroquine (CQ, 50 µM, MRGPRA3 agonist) as well as

217 ATP (1.25 mM) and/or ionomycin (Iono., 2 µM) as positive control. Bars indicate application
218 period; graphs represent mean (colored line) ± 95% confidence interval (in grey) of N cells
219 (n = 2). A waiting period of 45 min after the test stimulus was introduced to limit cross-
220 desensitization to NPFF, the continuous recording period 7–45 min was omitted for clarity.
221 Lower panel in C as in Fig.4F.
222